Technical Review

No. 2 · 1989

STSF—Practical instrumentation and application
Digital Filter Analysis: Real-time and Non Real-time Performance

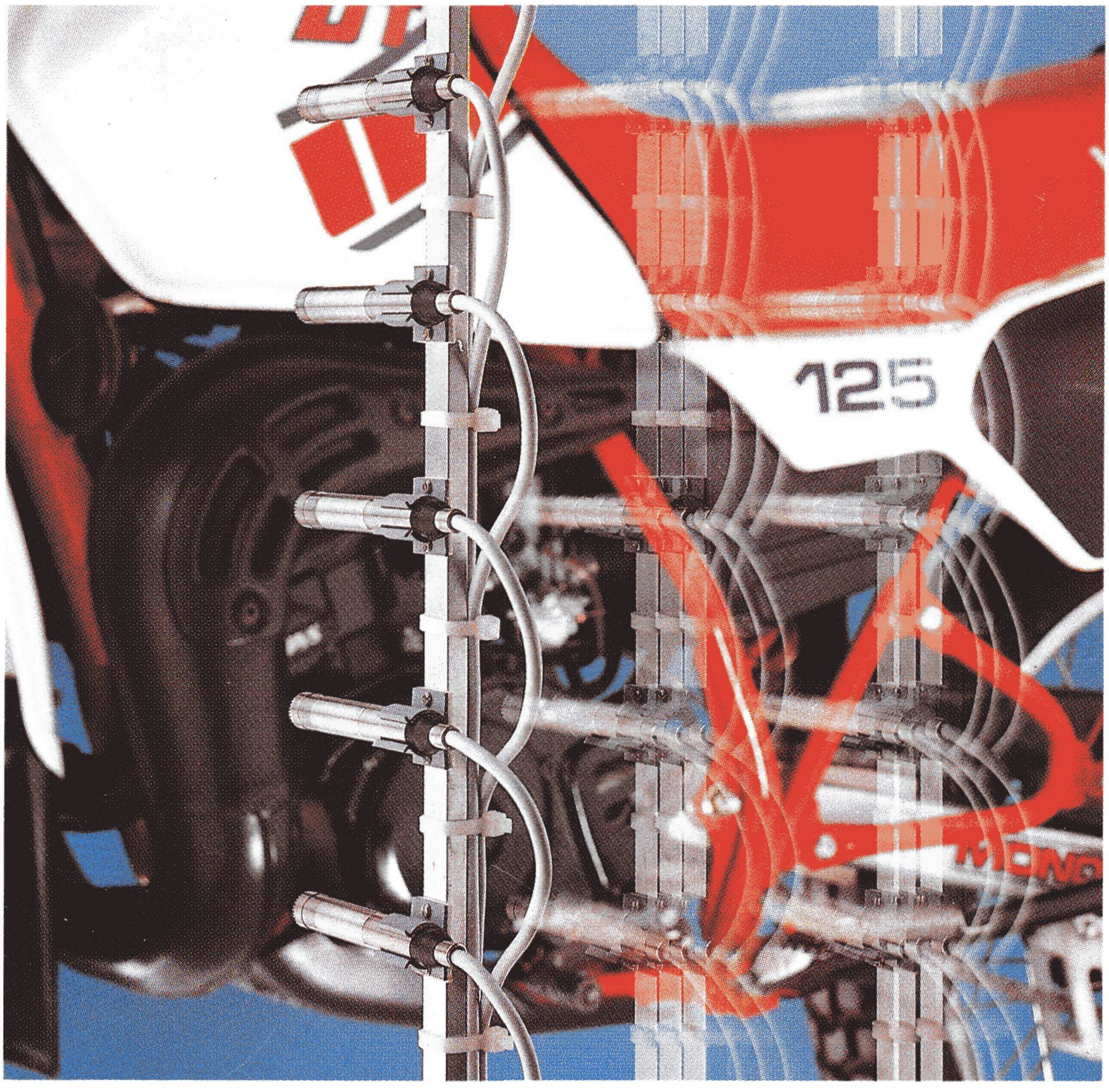

Brüel & Kjær

Previously issued numbers of Brüel & Kjær Technical Review

1–1989 STSF – A Unique Technique for scan based Near-field Acoustic Holography without restrictions on coherence
2–1988 Quantifying Draught Risk
1–1988 Using Experimental Modal Analysis to Simulate Structural Dynamic Modifications
Use of Operational Deflection Shapes for Noise Control of Discrete Tones
4–1987 Windows to FFT Analysis (Part II).
Acoustic Calibrator for Intensity Measurement Systems
3–1987 Windows to FFT Analysis (Part I)
2–1987 Recent Developments in Accelerometer Design
Trends in Accelerometer Calibration
1–1987 Vibration Monitoring of Machines
4–1986 Field Measurements of Sound Insulation with a Battery-Operated Intensity Analyzer
Pressure Microphones for Intensity Measurements with Significantly Improved Phase Properties
Measurement of Acoustical Distance between Intensity Probe Microphones
Wind and Turbulence Noise of Turbulence Screen, Nose Cone and Sound Intensity Probe with Wind Screen
3–1986 A Method of Determining the Modal Frequencies of Structures with Coupled Modes
Improvement to Monoreference Modal Data by Adding an Oblique Degree of Freedom for the Reference
2–1986 Quality in Spectral Match of Photometric Transducers
Guide to Lighting of Urban Areas
1–1986 Environmental Noise Measurements
4–1985 Validity of Intensity Measurements in Partially Diffuse Sound Field
Influence of Tripods and Microphone Clips on the Frequency Response of Microphones
3–1985 The Modulation Transfer Function in Room Acoustics
RASTI: A Tool for Evaluating Auditoria
2–1985 Heat Stress
A New Thermal Anemometer Probe for Indoor Air Velocity Measurements
1–1985 Local Thermal Discomfort
4–1984 Methods for the Calculation of Contrast
Proper Use of Weighting Functions for Impact Testing
Computer Data Acquisition from Brüel & Kjær Digital Frequency Analyzers 2131/2134 Using their Memory as a Buffer
3–1984 The Hilbert Transform
Microphone System for Extremely Low Sound Levels
Averaging Times of Level Recorder 2317
2–1984 Dual Channel FFT Analysis (Part II)

(Continued on cover page 3)

Technical Review

No. 2 · 1989

Contents

STSF–Practical instrumentation and applications 1
by Kevin B. Ginn & Jørgen Hald

Digital Filter Analysis: Real-time and Non Real-time Performance 28
by Svend Gade

STSF–Practical instrumentation and applications

Kevin B. Ginn & Jørgen Hald

Abstract

The Spatial Transformation of Sound Fields (STSF) technique involves a scan using an array of transducers over a (planar) surface close to the source under investigation. From cross spectra measured during the scan, a principal component representation of the sound field is extracted. Any power descriptor of the near field (intensity, sound pressure, etc.) can then be investigated by means of Near-field Acoustic Holography (NAH), while the more distant field can be determined by application of Helmholtz' integral equation.

The theoretical foundation of the cross spectrum principal component technique implemented in STSF has been discussed by J. Hald in [1] and the advantages of STSF compared to a number of acoustical holography techniques have been demonstrated. In this article, the practical implementation of STSF is discussed and some applications are described.

Sommaire

La technique de transformation spatiale des champs sonores (Spatial Transformation of Sound Fields) est fondée sur le balayage d'une surface plane près de la source étudiée. Une représentation de la composante principale est extraite de l'interspectre mesuré pendant le balayage. Tout descripteur de puissance du champ proche (intensité acoustique, pression sonore, etc.) est étudié par holographie acoustique du champ proche (Near-field acoustic holography), alors que le champ plus distant est déterminé par l'équation intégrale de Helmholtz.

Le fondement théorique de la technique de composante principale interspectrale employée en STSF a été couvert par J. Hald [1], et les avantages de la STSF sur diverses techniques holographiques ont été démontrés. Cet article décrit sa mise en application et en discute quelques exemples.

Zussammenfassung

Für die räumliche Transformation von Schallfeldern (Spatial Transformation of Sound Fields — STSF) wird mit einer Reihe von Aufnehmern eine ebene Fläche nahe der Schallquelle abgetastet. Das gemessene Kreuzspektrum repräsentiert die Hauptkomponenten des Schallfelds. Alle Leistungsparameter des Nahfelds (Intensität, Schalldruck usw.) können mit der akustischen Nahfeldholographie (NAH) untersucht werden. Für das fernere Feld wird die Helmholtz'sche Integralgleichung benutzt.

Die Theorie der Kreuzspektrum-Hauptkomponententechnik für STSF sowie die Vorteile von STSF gegenüber anderen akustischen Holographie-Verfahren werden in [1] von J. Hald diskutiert. Der Artikel beschäftigt sich mit der praktischen Anwendung von STSF und beschreibt einige Beispiele.

1. Principle of STSF

The basic principle of the Spatial Transformation of Sound Fields (STSF) technique is illustrated in Fig. 1. Based on cross spectra measured over a planar surface close to the source under investigation, all parameters of the sound field can be mapped over a three dimensional region extending from the surface of the source to infinity. The near field is predicted from the scan data using Near-field Acoustic Holography (NAH), while the more distant field is calculated using Helmholtz' Integral Equation (HIE).

In addition to the 3D mapping capability based on 2D measurements, STSF also provides the possibility of doing Partial Source Attenuation Simulation (PSAS). This simulation is done by backwards propagation of the cross spectral representation of the sound field from the measurement surface to (ideally) the source surface, then modifying the representation at the source surface according to an attenuation model and finally predicting the sound field from the modified representation.

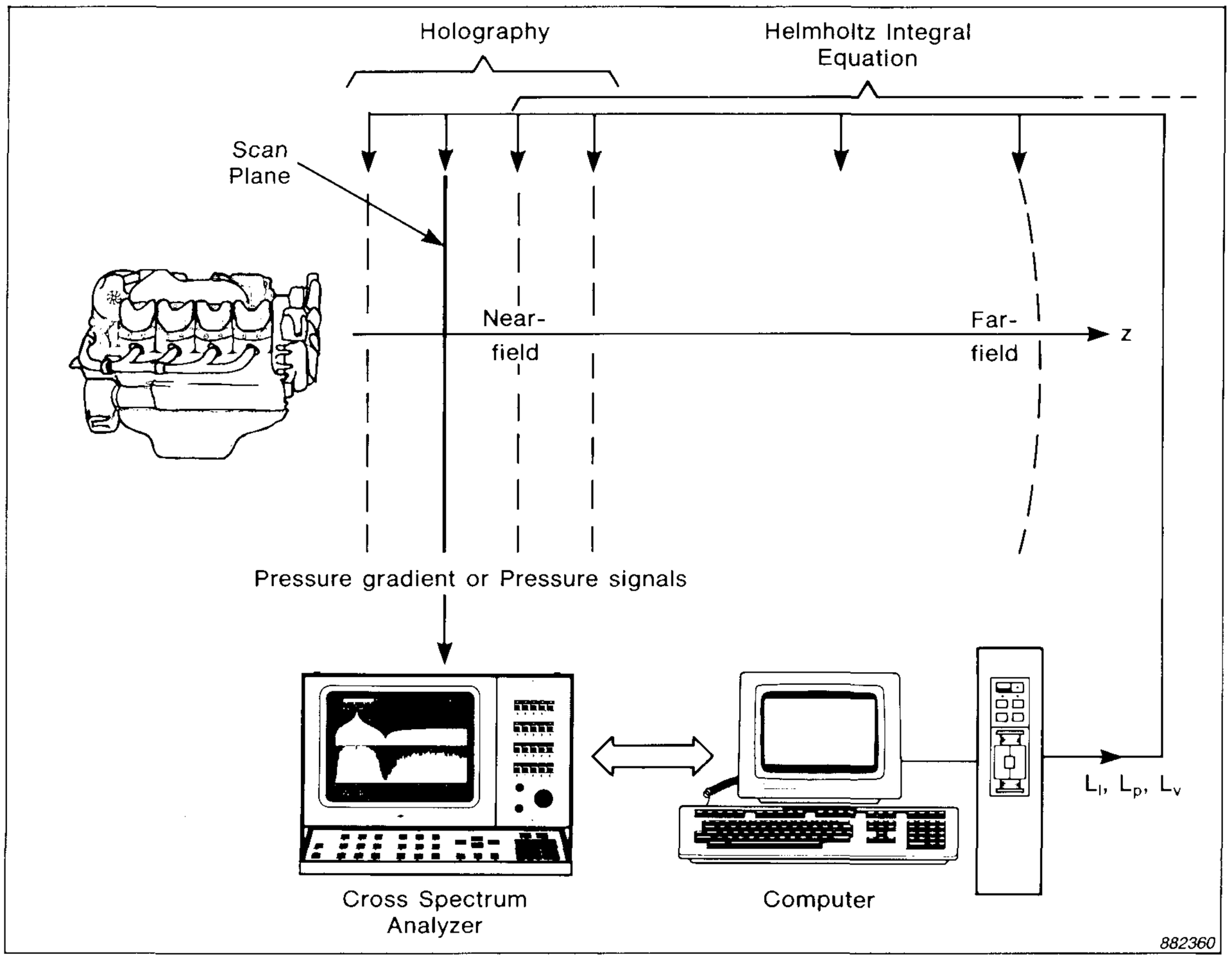

Fig. 1. Principle of STSF

2. Instrumentation

The instrumentation for STSF can vary greatly for different applications. Two standard systems, based on a 2-channel FFT analyzer and a dual channel, real-time frequency analyzer, are depicted in Fig. 2.

The main parts of the STSF instrumentation are:

1. Transducers
2. Cross spectrum analyzer
3. Controller, data storage and post processing.

2.1. Transducers

The planar scan over the measurement area involves the measurement of pressure signals or particle velocity signals. The pressure signals can be measured using an array of ordinary B & K microphones of the same type,

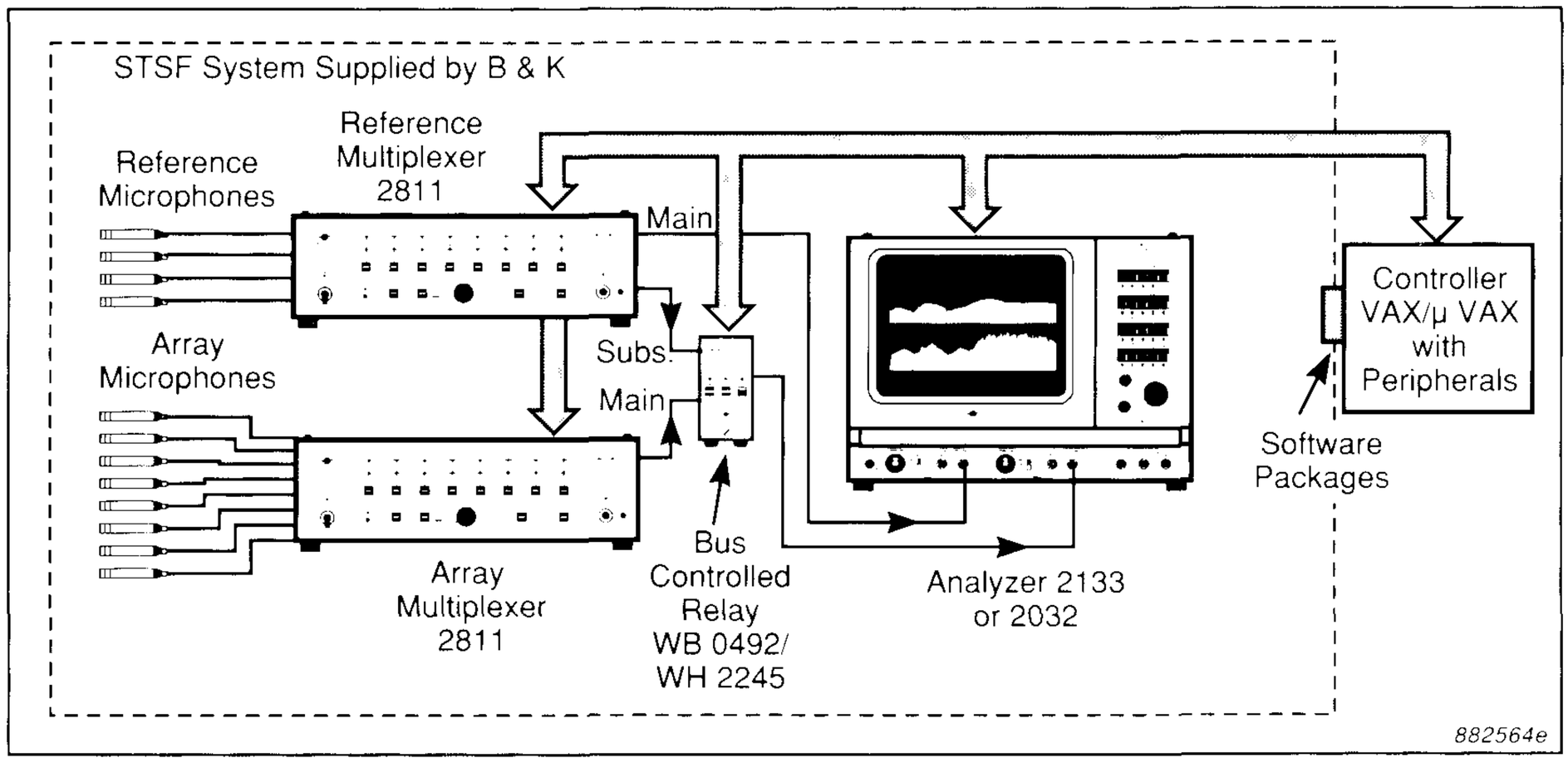

Fig. 2. STSF System Type 9606 with 2032 or Type 9607 with 2133

no phase matching between the individual microphones being necessary. The particle velocity signals can be determined from a finite difference approximation using an array of phase matched pairs of microphones. The difference between the signals from the front and the rear microphones of the pairs is determined directly from the analogue signals by one of the scan multiplexers.

If one is only interested in the far field in a horizontal plane then a far quicker measurement can be performed by summing the outputs from each column of microphones in real time thus effectively treating the column of scan microphones as a single transducer. This summation is performed by the scan multiplexer. The measurement time is reduced by a factor equal to the number of scan microphones.

The reference microphones should be placed between the sound source and the scan plane and should be well distributed over the scan area so that from every scan position there is always at least one reference microphone within one correlation length [4]. This distance is set by the bandwidth being used. For third octaves a correlation length is about two wavelengths. For twelfth octaves it is about eight wavelengths. A greater distance than the correlation length will result in a poorer representation of the sound field over the scan area, i.e. a poorer representation of the large cross spectrum matrix. Preferably the correlation length should be sufficiently large to include the entire scan area from a single reference.

In the systems depicted in Fig. 2 the cross spectra are measured using a column of scan microphones and an array of reference microphones. The

number of microphones in a practical set-up need not be excessively large. In fact the minimum number of transducers required is two, one reference and one scan transducer. A practical application using STSF in situ with only two transducers to investigate the noise radiated by a seismic survey lorry is described in Ref. [2].

Instead of reference microphones other transducers could be employed e.g. accelerometers mounted on the source, pressure transducers inside an engine's cylinder, an electrical signal from say a vibration exciter. The advantages of using a transducer such as an accelerometer on the test object itself are firstly that the influence of background noise on the measurement can be considerably reduced and secondly one can position the accelerometers directly on the suspected source. For delicate or very hot sources a non-contact laser vibrometer could be used. A disadvantage is that an accelerometer placed close to a node line would give little or no signal. A sound pressure field rarely has corresponding node lines. Thus relatively more reference accelerometers than microphones need to be used to completely represent the sound field radiated from a structure [3].

2.2. Cross spectrum analyzer

In theory any cross spectrum analyzer could be employed for STSF. Three systems have been developed by Brüel & Kjær, based on three analyzers:

- Sound Intensity Analyzer 2134
- Dual Channel Real-time Frequency Analyzer 2133

Three basic STSF systems

	Bandwidth	No. of Channels	Frequency range
CPB	23% (2134 & 2133)	15 · 1/3 octave	Typically 80 Hz to 2 kHz
	6% (2133)	60 · 1/12 octave	Typically 125 Hz to 3,15 kHz
FFT	1 Hz (2032)	24	4 Hz to 24Hz
	2 Hz (2032)	24	8 Hz to 48 Hz
	5 Hz (2032)	39	20 Hz to 195 Hz
	10 Hz (2032)	39	40 Hz to 390 Hz
	20 Hz (2032)	39	80 Hz to 780 Hz
	50 Hz (2032)	31	200 Hz to 1550 Hz
	100 Hz (2032)	31	400 Hz to 3100 Hz
	200 Hz (2032)	31	800 Hz to 6200 Hz

T02299GB0

Table 1. Frequency ranges of the three STSF Systems

- Dual Channel Signal Analyzer 2032 high speed version. The 2034 standard version could also be used but is not to be recommended as the measurement time would become excessively long.

The main features of the three systems are given in Table 1.

2.3. Controller, data storage and post-processing

For the original STSF system based on a modified Sound Intensity Analyzer 2134, the measurement is controlled by the Graphics Recorder Type

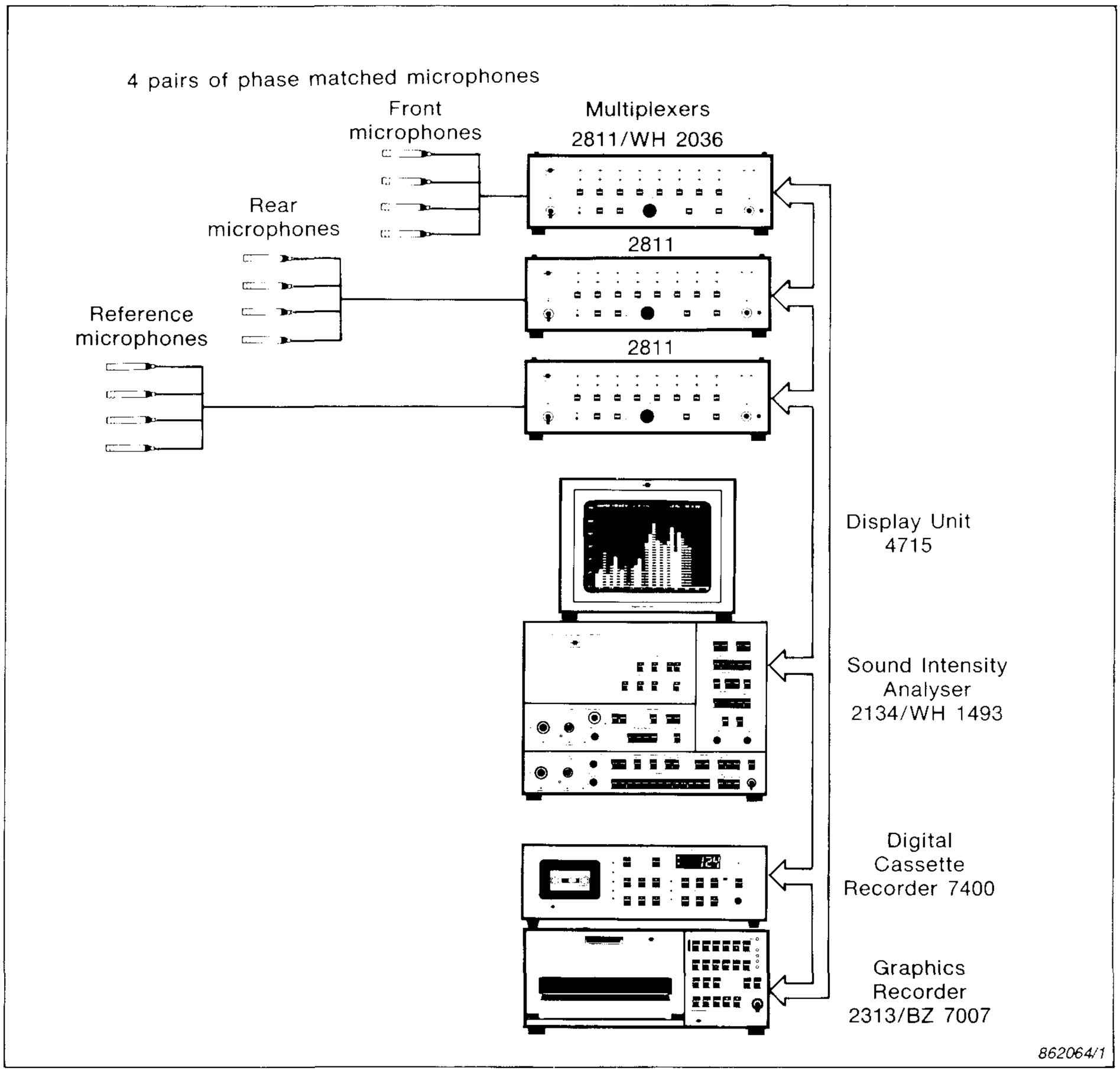

Fig. 3. STSF system based on Sound Intensity Analyzer Type 2134 modified to measure cross spectra. The instrumentation here is set-up to measure particle velocity during the scan

2313 fitted with a dedicated Application Package BZ 7007. Data is stored on a Digital Cassette Recorder 7400 then transferred to a VAX/micro VAX for holographic post-processing (Fig. 3).

For STSF Systems Type 9606 and 9607 based on analyzers 2032/34 and 2133 respectively, a micro VAX II or VAX station II is used as the controller and post-processor. A full STSF software package for VAX based systems consists of two parts:

1. Control and data acquisition
2. Calculation and plot.

The menu-driven control part includes a number of inspection functions which enables the validity of the data to be checked before proceeding to the STSF calculations. Measurement errors such as too few or poorly positioned reference transducers, too short averaging times, or spurious data, can thus be detected. If necessary, new measurements can be made and substituted into the original data set.

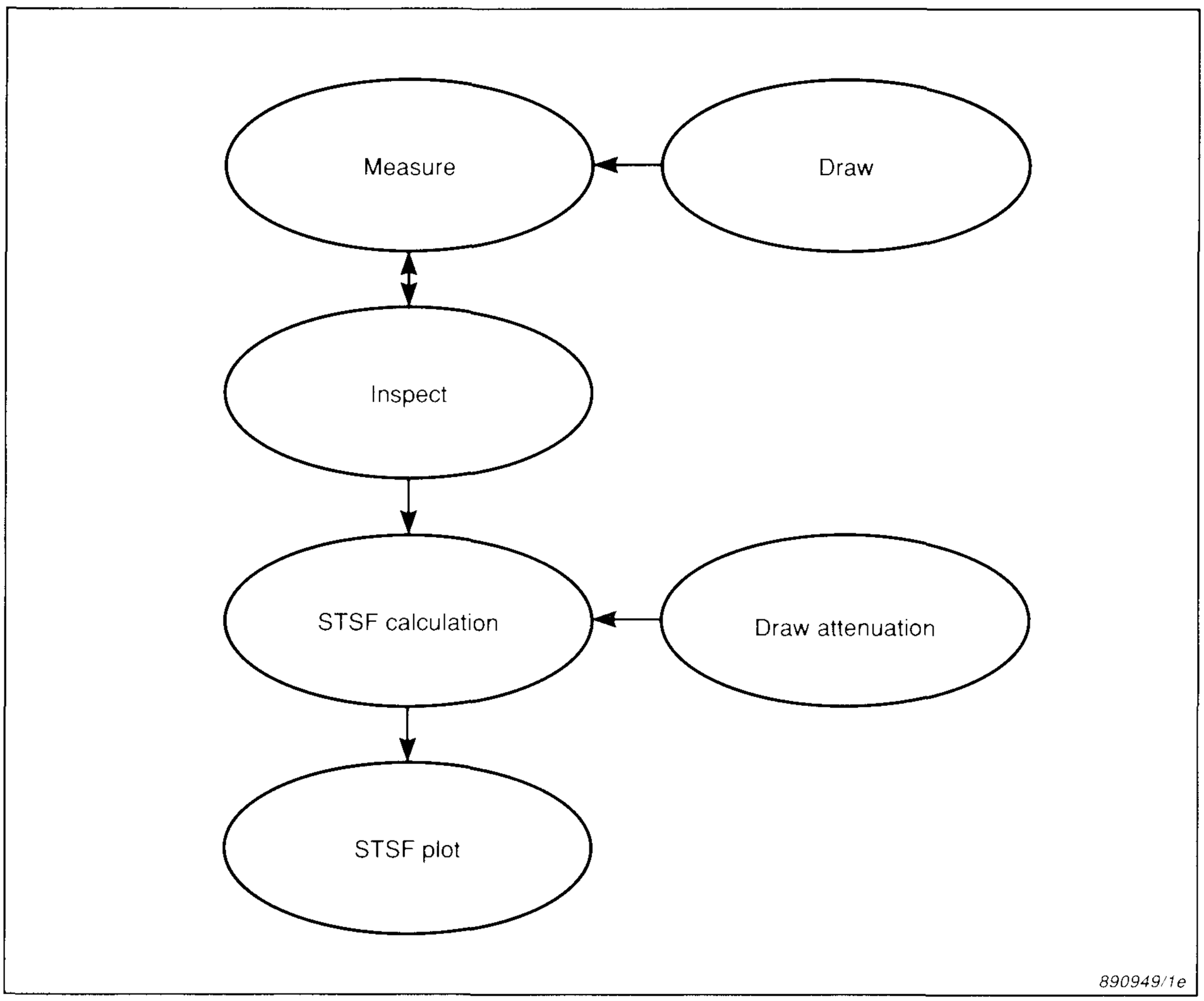

Fig. 4. Flow diagram for STSF measurements

A series of prompts, warnings, menus and a recurring overview of the hard key functions guide the user through the measurement and calculation procedures.

In the standard calculation and plot program the following possibilities are available.

1. Sound pressure level along a line
2. Sound pressure spectrum at a specified position
3. Sound power spectrum
4. Acoustical holography
5. Contour plots of: pressure, active intensity, reactive intensity, particle velocity, radiation pattern
6. Simulation of source attenuation.

In addition, a number of supplementary programs can be offered including:

1. Drawing the test object on the contour plots.
2. Plotting vector intensity diagrams.
3. Measuring and plotting programs using separable co-ordinate systems other than Cartesian.

A simplified flow diagram of the processing of STSF measurements is shown in Fig. 4.

3. Measurement Procedure

Good results require well defined measurement conditions. The measurement set-up is described by a set of parameters (e.g. type of probe used, number of references, measurement grid size, environmental conditions, presence of reflective plane) which are keyed into the computer by the user. A typical set-up is shown in Fig. 5.

The most important decisions for the user concern the geometry of the measurement. The starting point is the frequency range of interest. The spacing between the scan microphones is closely related to the upper frequency of interest. There must be at least two microphones per wavelength at this upper frequency in order to avoid spatial aliasing. The size of the scan area then has to be set. This area must adequately cover the source as shown in Fig. 6, otherwise the basic hypothesis that practically all the energy of the sound field radiated into the measurement half-space passes through the measurement window, will no longer be valid.

The distance from the scan microphones to the source should be approximately equal to but not less than, one inter-scan-microphone distance in order to avoid spatial aliasing. At this distance, the amplitudes of the un-

Press F10 to Quit. Press F14 to Exit.

Measurement Setup

2133 Measurement No.: 1 **Date: 11-APR-89.** **Title: XXXX**

Text No. 1: Bruel & Kjaer
Text No. 2: STSF Measurement
Text No. 3: Default Setup
Text No. 4:

Temperature	:	20.0 C	Avg. time in ref.meas.	:	4.00 sec
Humidity	:	60.0 %	Avg. time in cross meas:		2.00 sec
Static pressure	:	101000.Pa	Avg. time in auto meas.:		2.00 sec
Array probe type	:	Pressure	Measurement bandwidth.	:	1/3 oct
			Lowest frequency	:	50 Hz
Array mux. output	:	Mux	Highest frequency	:	1.25 kHz
Measurement condition	:	Free Field			
			Ground plane distance	:	1.00 m
No. of ref.transducers	:	1	Scan plane tilt	:	0.0 deg
No. of array probes	:	8	Distance source centre	:	0.20 m
No. of traverses	:	1	Distance source surface:		0.10 m
No. of traverse pos.	:	10			
Spacing in X direction	:	0.07 m	Stationarity check ref.:		1
Spacing in Y direction	:	0.07 m	Background noise :		Insignificant

Temperature in Celsius. Valid range: -20.0 - 100.0

891662

Fig. 5. Typical STSF measurement set-up

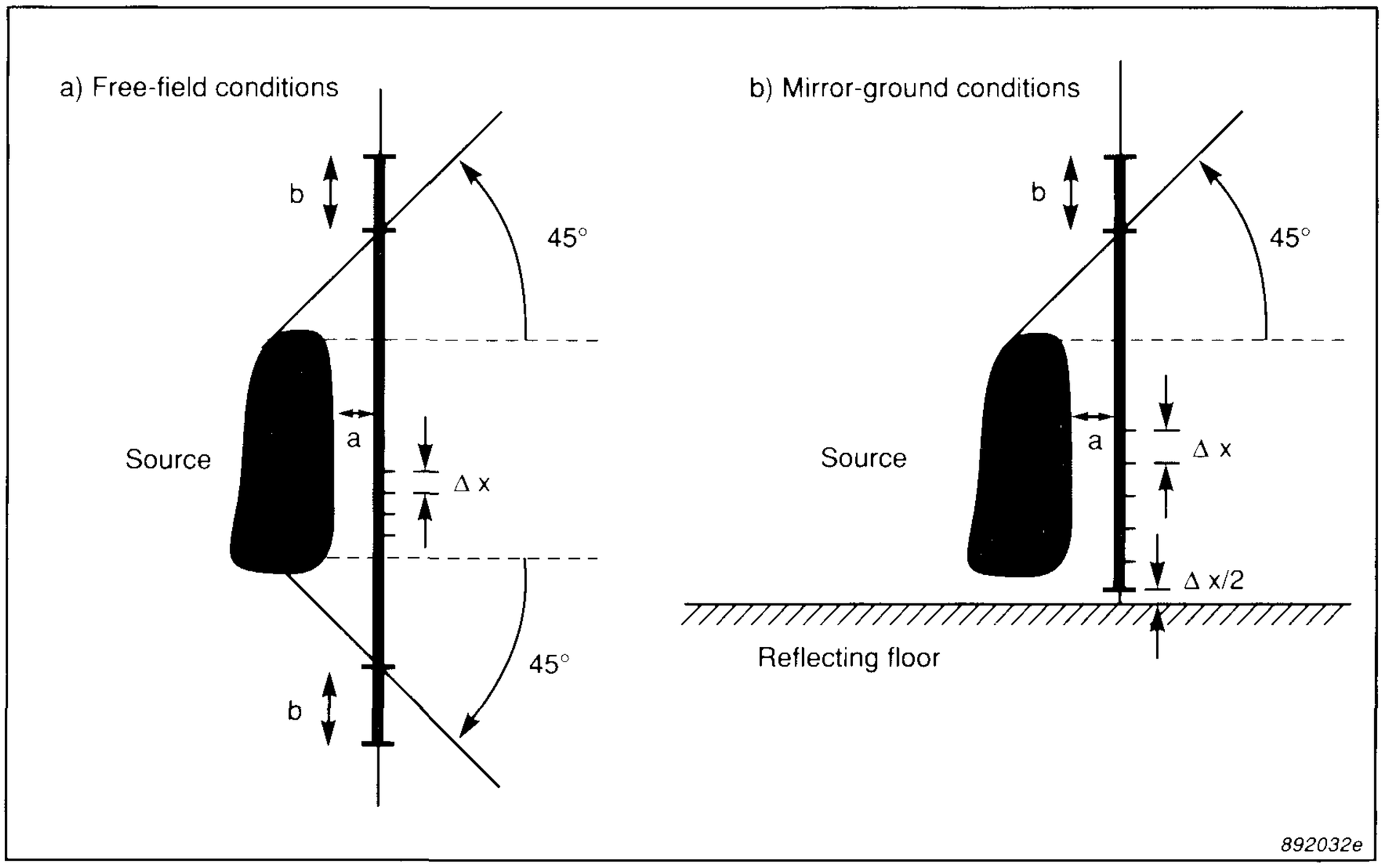

Fig. 6. Determination of the size of the scan area for a) free field conditions b) mirror ground conditions. The distances $a \approx \Delta x$ and $b \geqslant 3\ \Delta x$. Also $b \geqslant \lambda/8$

der sampled evanescent waves have decayed by approximately 20 dB from the source surface. If measurements were attempted at significantly greater distances from the source then the exponentially decaying evanescent waves (the waves necessary to describe the details of the sound field) would be swamped by the background noise level.

If a reflecting ground surface is present, then measurements must be made right down to the ground. The positioning of the scan microphones is critical because for the calculations an image source is created using the floor as the plane of symmetry. Thus unless the first scan microphone is positioned exactly one half an inter-scan-microphone spacing above the floor, the plots resulting from the subsequent calculations will be distorted.

3.1. Inspection of measured data

The Inspect function of the STSF program packages is used to verify and obtain plots of the measured data and also to check the validity of the data. The validity check is performed using the following three functions:

1) Validation: To check the representation of the field at scan and reference positions.
2) Eigenvalue spectrum: To plot the eigenvalue spectrum for the reference signal cross spectrum matrix.
3) Stationarity check: To check the stationarity of a selected reference signal during the scan.

In the Validation function the field representation is checked by comparing the measured sound pressure level to the level calculated from the measured cross spectra. With one reference, the difference between the two pressure levels expresses the coherence between the array microphone signal and the reference signal. With several references, the difference represents a multiple coherence. Provided a sufficient set of references is employed, the multiple coherence is close to one or equivalently, the difference between the measured and the represented sound pressure level is small at all scan positions.

There will always be some discrepancy between the measured and calculated spectra at the scan microphone positions. In general at low frequency this deviation will be mainly due to too short an averaging time, and the high frequency deviation will be mainly due to an insufficient number of references or to a poor positioning of the references. The deviation will be

smallest in regions close to the references. Non-stationarity of the source signals will tend to create discrepancies at all frequencies.

In practice the validation procedure should be performed before a complete scan is made. This can be accomplished by initially taking measurements only at the set of array positions where the measured and the represented pressure levels are to be compared. By doing so, one avoids spending time taking complete measurements only to obtain bad data.

Good measurements may be obtained in environments with severe uncorrelated background noise by positioning the references very close to the source. This means that the cross spectra and thus all STSF calculations will be unaffected by the background noise. Since, however, the measured autospectra (pressure) will be affected, the above validation procedure does not apply.

The Eigenvalue spectrum function shows how many significant independent partial sources the reference measurement (cross spectra between every pair of references) has identified for each frequency band. Each eigenvalue represents the autopower of a virtual independent partial source. Thus, all eigenvalues should be non-negative; the occurrence of negative eigenvalues is due to non-stationarity of the source during the reference measurement or use of too short an averaging time. If large negative eigenvalues are observed, the source has probably been very non-stationary during the reference measurement, which is not acceptable. If nothing can be done to improve the stationarity of the source then the reference measurement should be repeated using a longer averaging time.

Stationarity during the scan is also important, although not as critical as during the reference measurement. To be able to check the stationarity during scan, the autospectrum at a specified reference is measured and stored for each position of the array. After the scan, the variation of this reference autospectrum during the scan, can be compared with the value obtained during the reference measurement by means of the Stationarity Check function.

4. Applications

Practical applications of STSF can be found in many branches of industry and in the automotive industry in particular. Here the engine group, transmission group and whole vehicle group could all apply STSF in their work. The engine group for example, would be particularly interested in the acoustical holography capability for source location during the development of new products. The whole vehicle group would be interested in the

calculation of radiation patterns as a way of quantifying the noisiness of a vehicle. Tyre manufacturers are interested in the radiation characteristics of various tyre profiles. The aeronautic and building industries are interested in the transmission paths via elements such as windows and doors. Some practical measurements are described below.

4.1. Measurement on a Motorcycle

The measurement was performed using the narrowband system Type 9606, over the right-hand side of an idling motorcycle situated on a quiet road. Eleven microphones were scanned over 14 measurement positions, the distance between each scan position being 7 cm. Thus the total scan area was 98 cm × 77 cm, Fig. 7. The scan plane was situated at 10 cm from the crankshaft cover (Fig. 8). Five reference microphones were employed. The total measurement time was 30 min. As the motorcycle was inclined during the measurement and as the engine was relatively far from the ground, it was judged that reflections from the ground had little influence

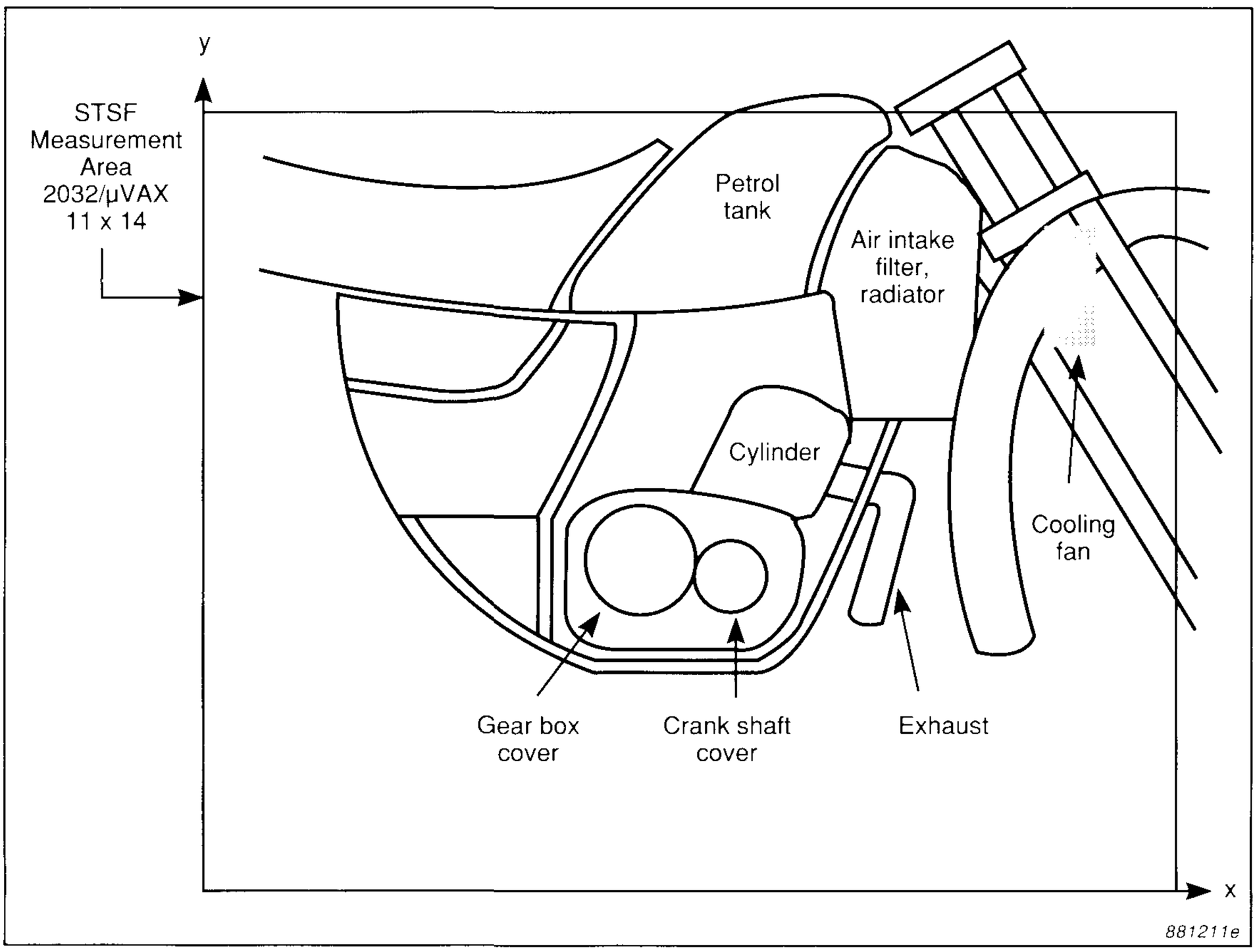

Fig. 7. Position of STSF measurement area on the motorcycle

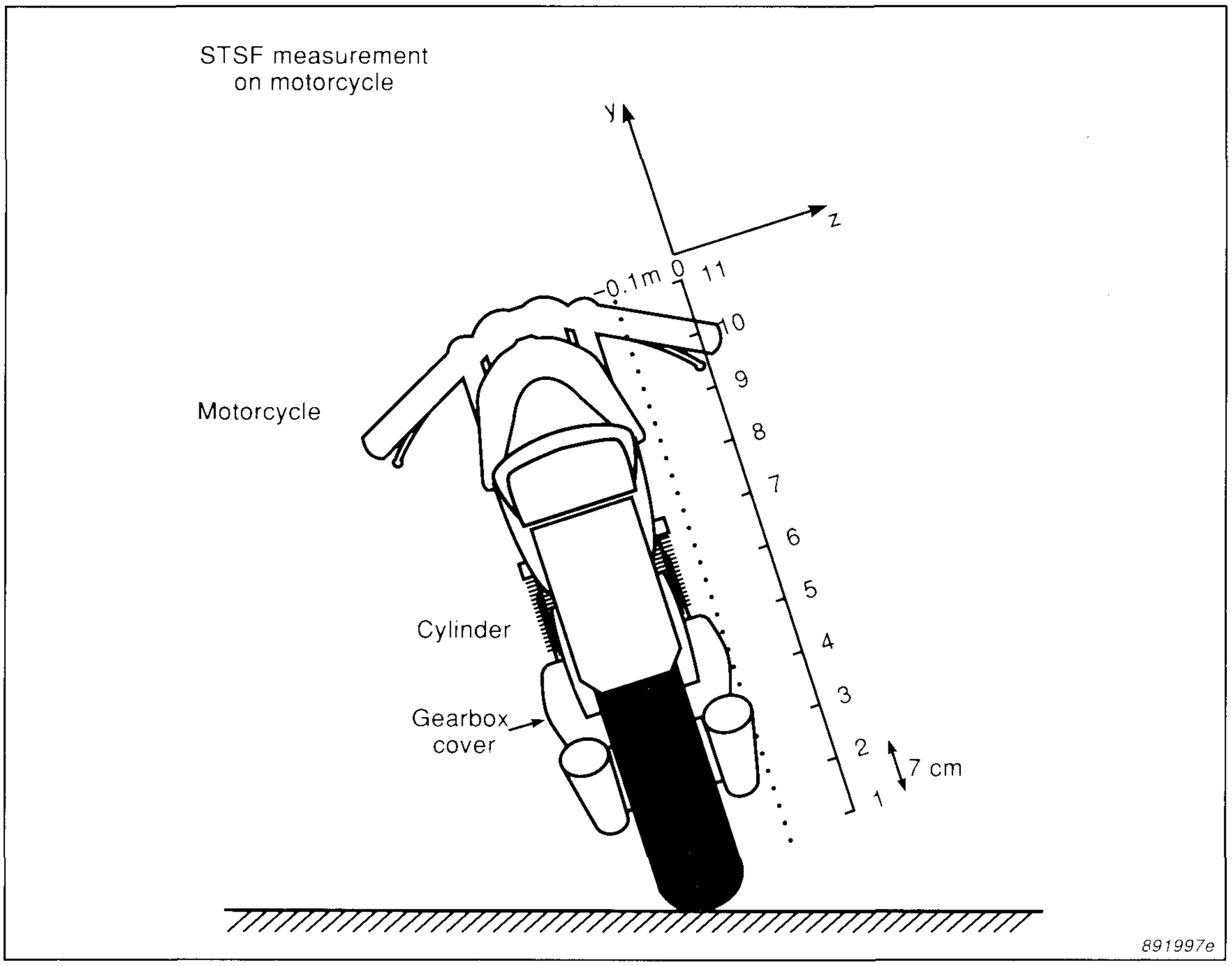

Fig. 8. Position of the microphone array relative to the motorcycle

on the noise which propagated from the engine and through the measurement window. Thus in the subsequent calculations free-field propagation was assumed. Figures 9 to 13 show contour maps of pressure, active intensity and reactive intensity as calculated by the near-field holography technique. All results are for a 100 Hz band centred on 1600 Hz. The parameters listed to the right of the plots are for conditioning the data by means of windows, spatial filters and dynamic ranges before performing the calculations. A comparison of Figs. 9 and 10 shows that active intensity is a better indicator than pressure for locating the principal noise generating regions. The reactive intensity plot of Fig. 11 is even more revealing, pinpointing the crankshaft cover. The regions of negative reactive intensity (indicated by dotted contour lines on Fig. 11) indicate that the pressure gradient in these regions decreases as the motorcycle is approached i.e. as one passes through the radiation cone of the crankshaft cover. When trying to interpret such contour plots it should be remembered that regions

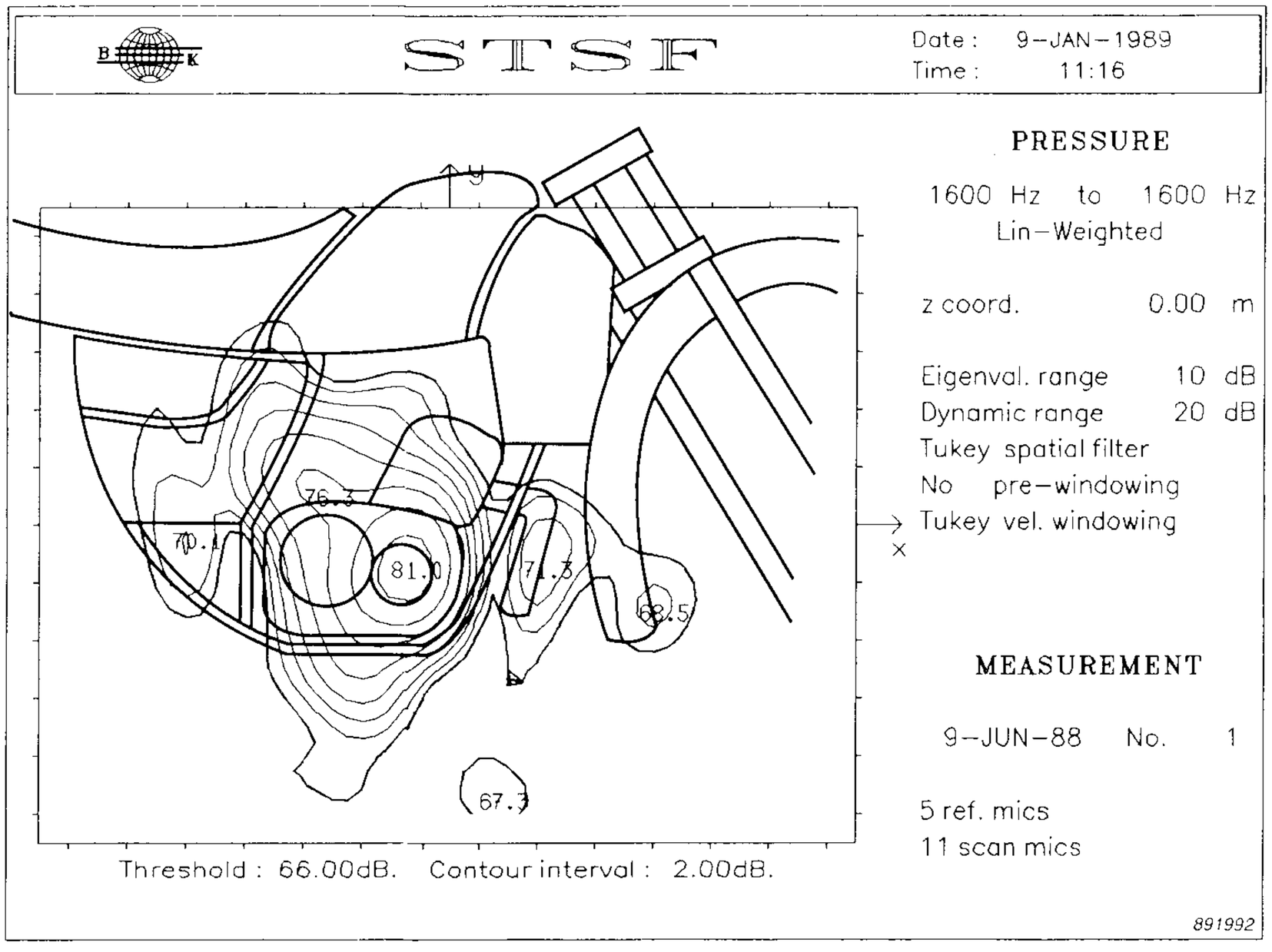

Fig. 9. Pressure contour map in the scan plane (z = 0 m)

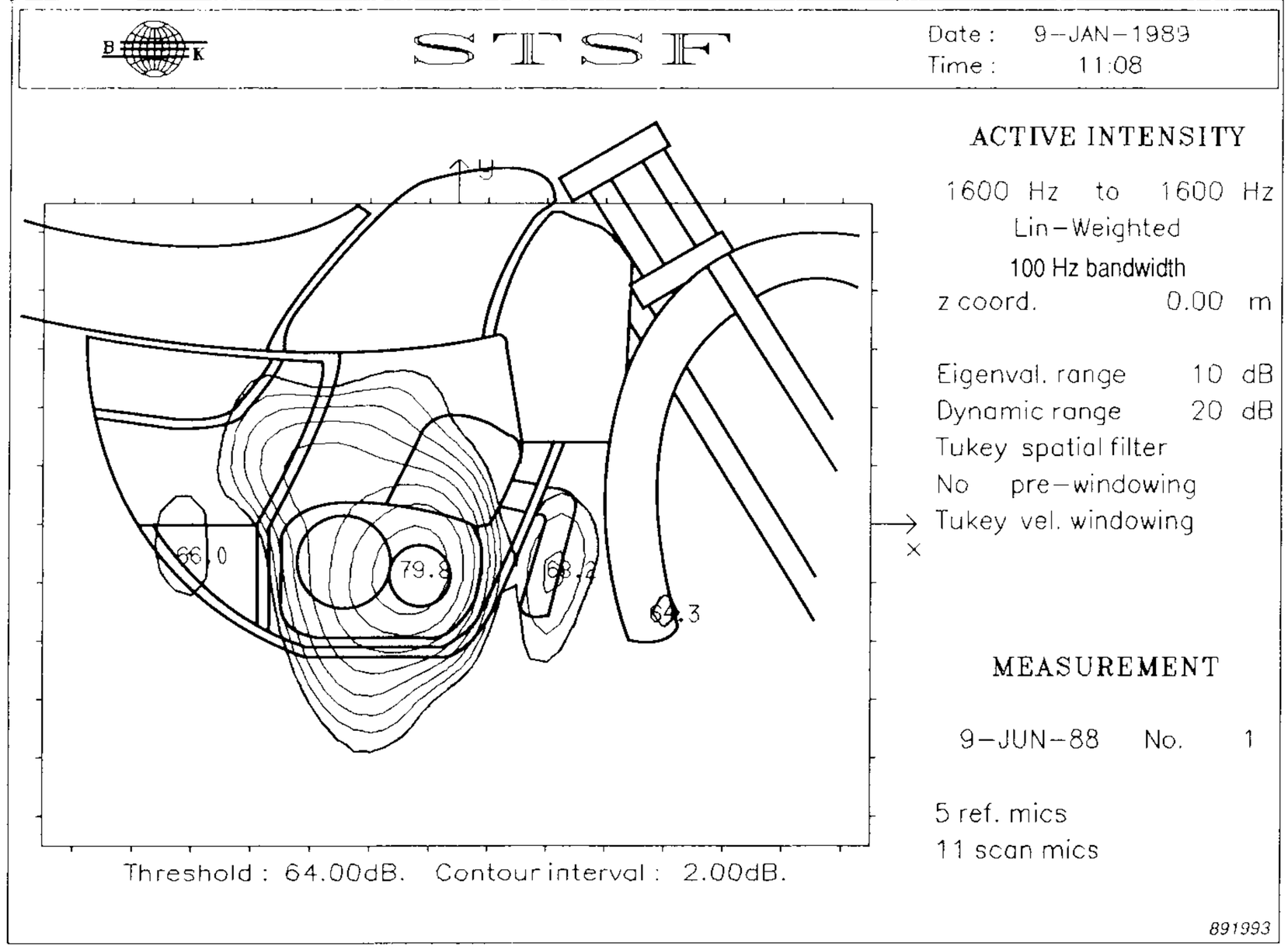

Fig. 10. Active intensity contour map in the scan plane (z = 0 m)

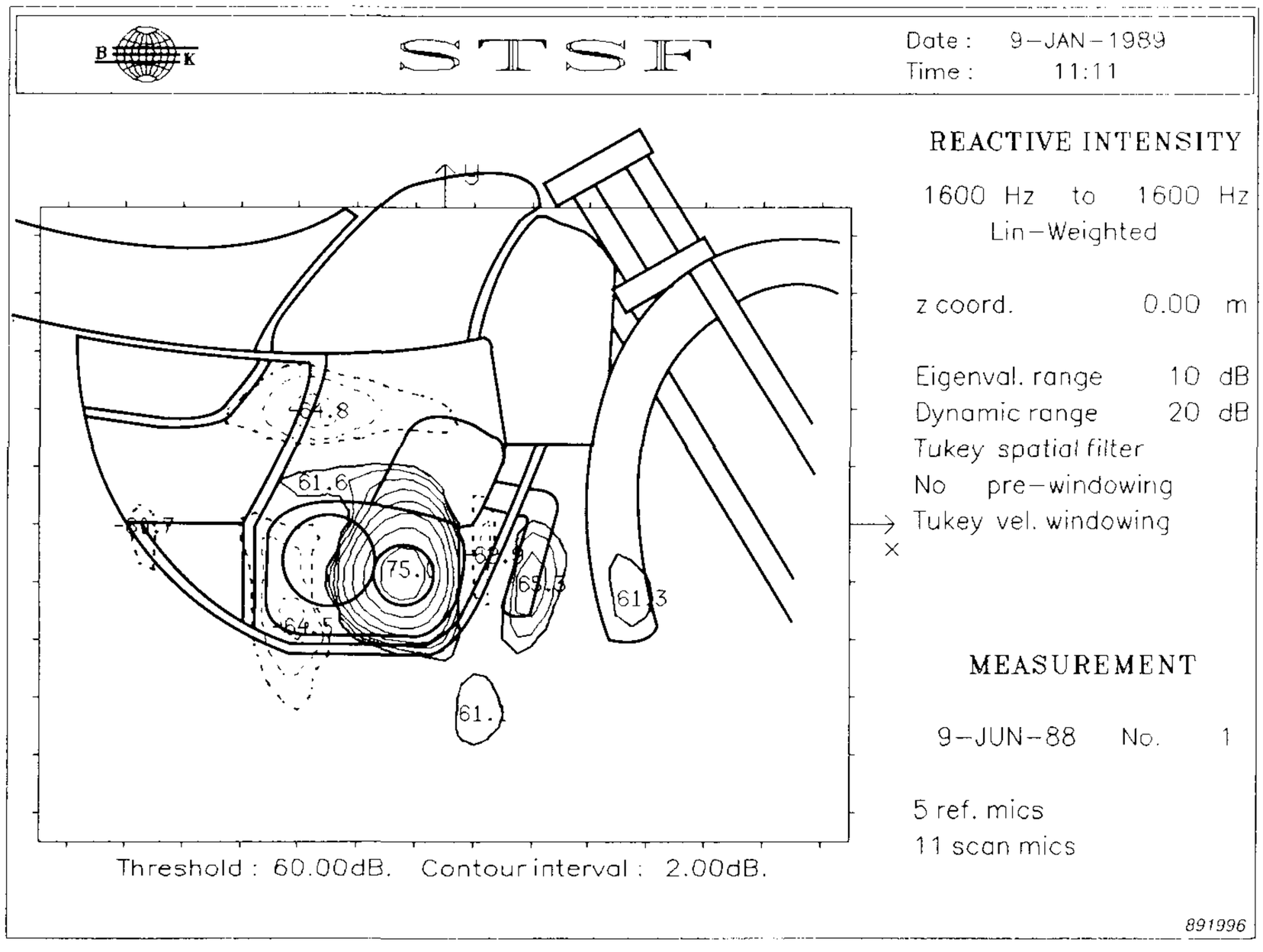

Fig. 11. Reactive intensity contour map in the scan plane (z = 0 m)

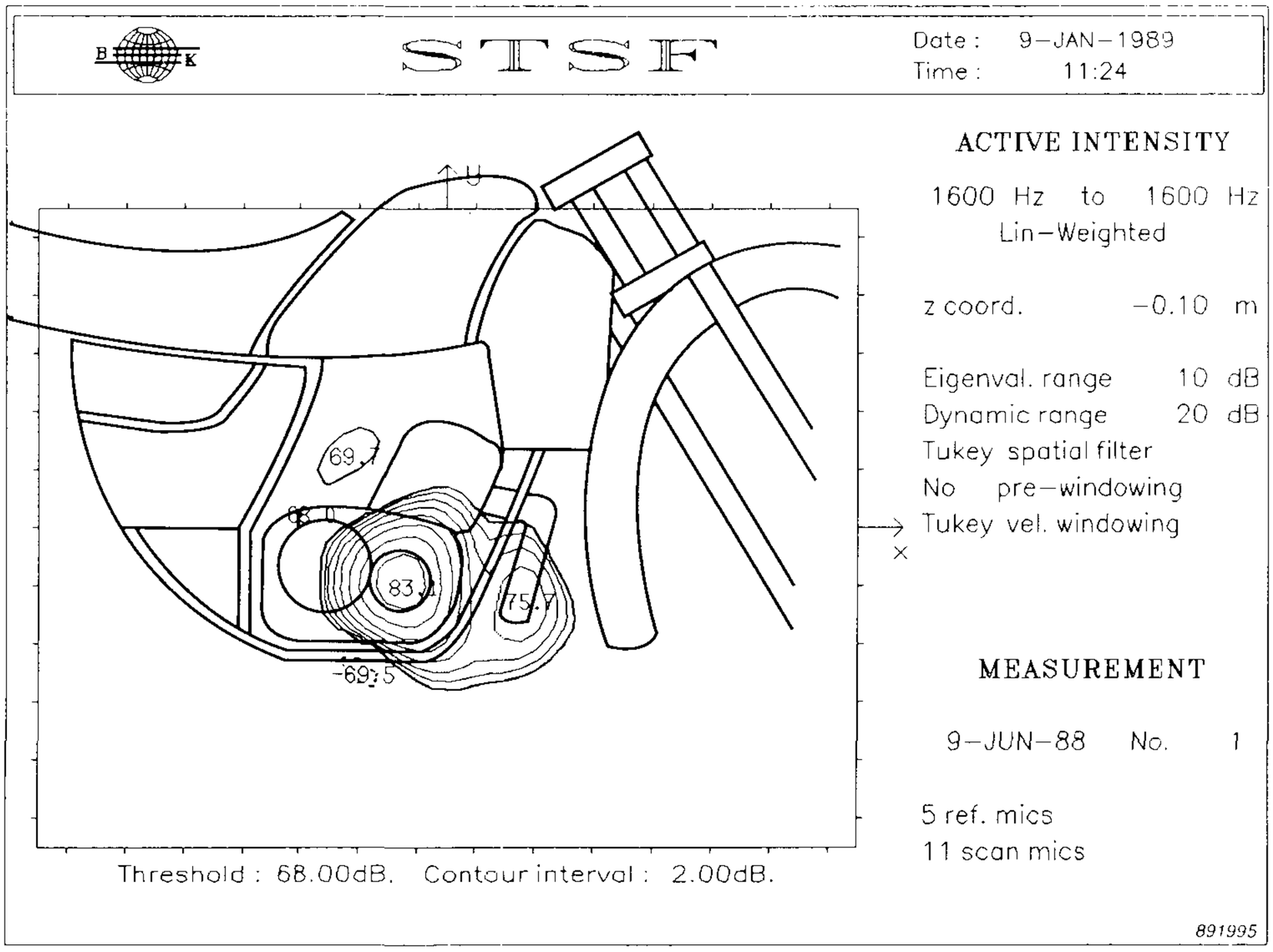

Fig. 12. Active intensity contour map 10 cm closer to the motorcycle (z = −0,1 m)

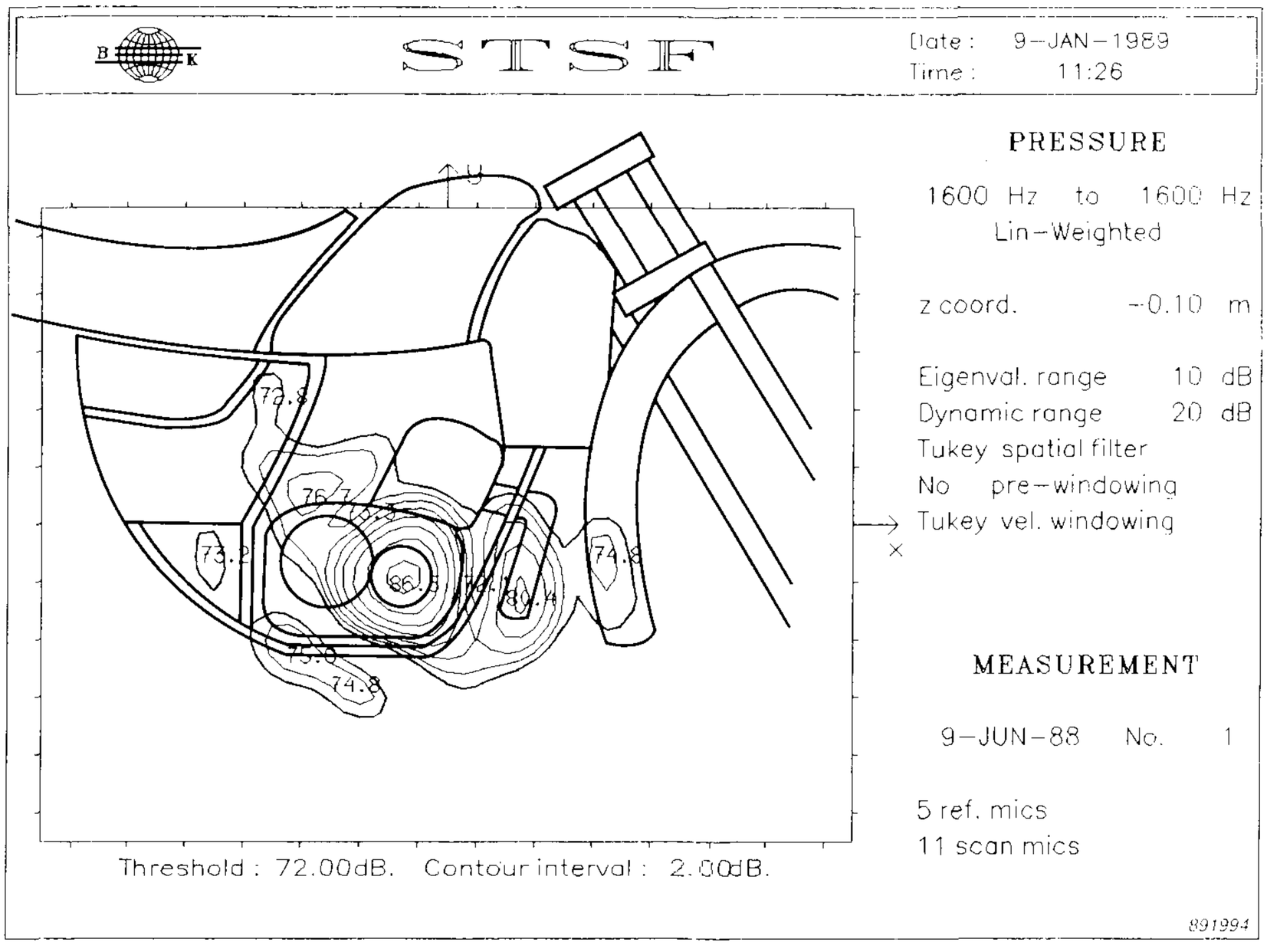

Fig. 13. Pressure contour map 10 cm closer to the motorcycle ($z = -0{,}1$ m)

of high reactive intensity do not necessarily indicate the presence of a sound source [4]. Plots of the various acoustical parameters should be used to complement one another when performing a noise survey. Figs. 12 and 13 show the contour plots of active intensity and pressure at 10 cm closer to the motorcycle, clearly indicating the ability of the STSF technique to "focus" on the sound source. It is interesting to note that in the scan plane the pressure-intensity index in front of the crankshaft box cover is about 2 dB whereas 10 cm closer to the engine the index has increased as one would expect to about 3,5 dB. In general, the closer one gets to a sound source the more complex the acoustical field becomes and the greater the pressure-intensity index.

4.2. Measurement on a Whole Vehicle

A measurement on a complete vehicle was performed using the 2134 third octave band system. Eight microphones were scanned over 32 positions over the right-hand side of an idling car situated in a semi-anechoic chamber. The total measurement time was 80 min. A calculation line was posi-

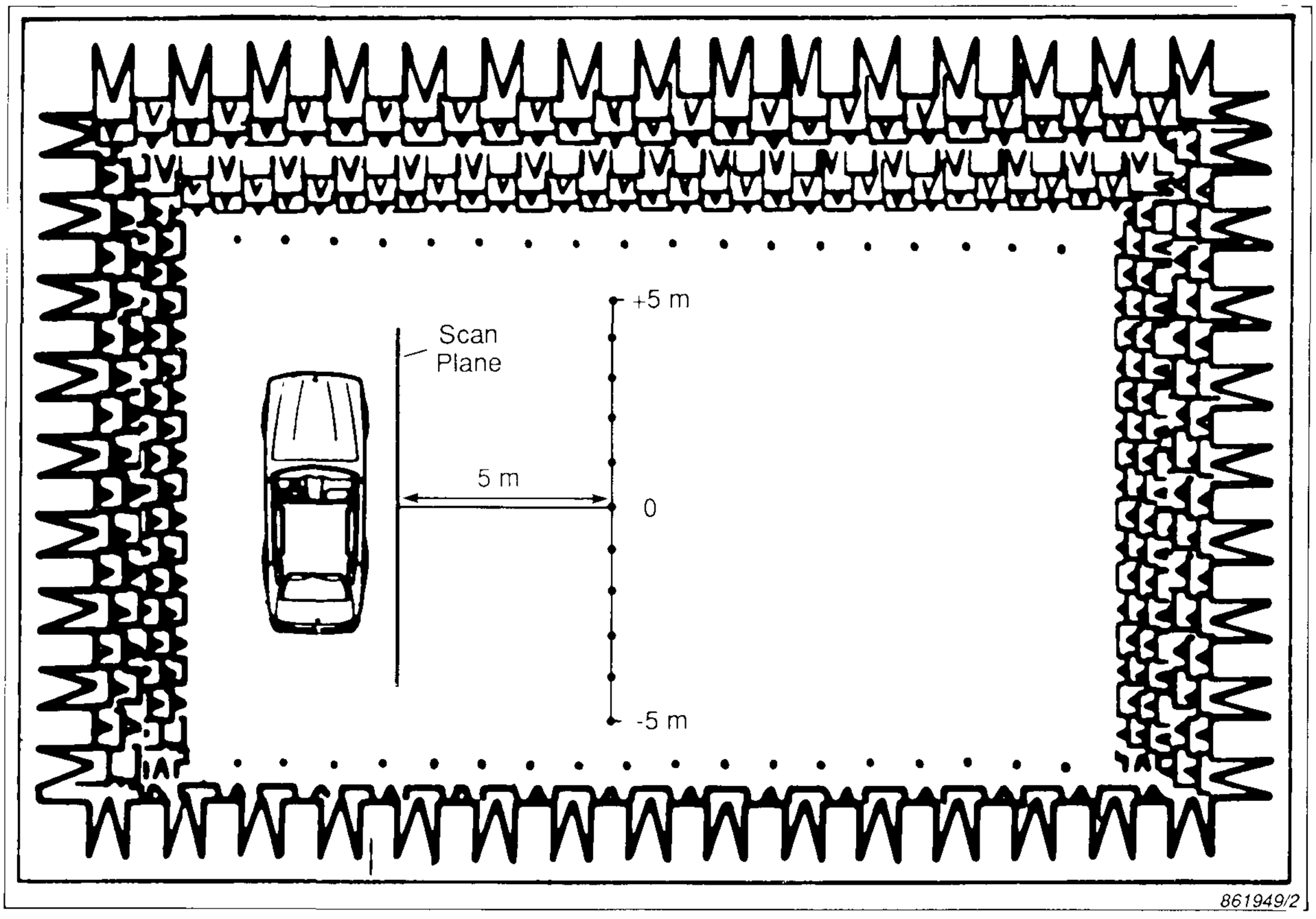

Fig. 14. Position of car in semi-anechoic test chamber with scan position and calculation/control line as indicated

tioned at 5 m from the scan plane, 1,16 m above the ground (Fig. 14). For the calculations it was assumed that the floor acted as a perfect reflector i.e. a mirror ground. The sound pressure level was calculated in the 80 Hz third octave band and the results compared with the level measured directly at 11 points along the line. The direct measurement was possible because the test chamber had extremely large dimensions, approximately 12 × 20 × 8 m, with a lower limiting frequency of 60 Hz. The agreement within a region of ± 2,5 m of the axis is within ± 0,5 dB (Fig. 15). Agreement in the ± 5,0 m range is within ± 2 dB. Higher accuracy is to be expected on axis whilst at the extremities of the line, errors due to a finite scan area and finite room dimensions start to influence the results. For a discussion of the effect of bandwidth on the measured results see [4] & [5].

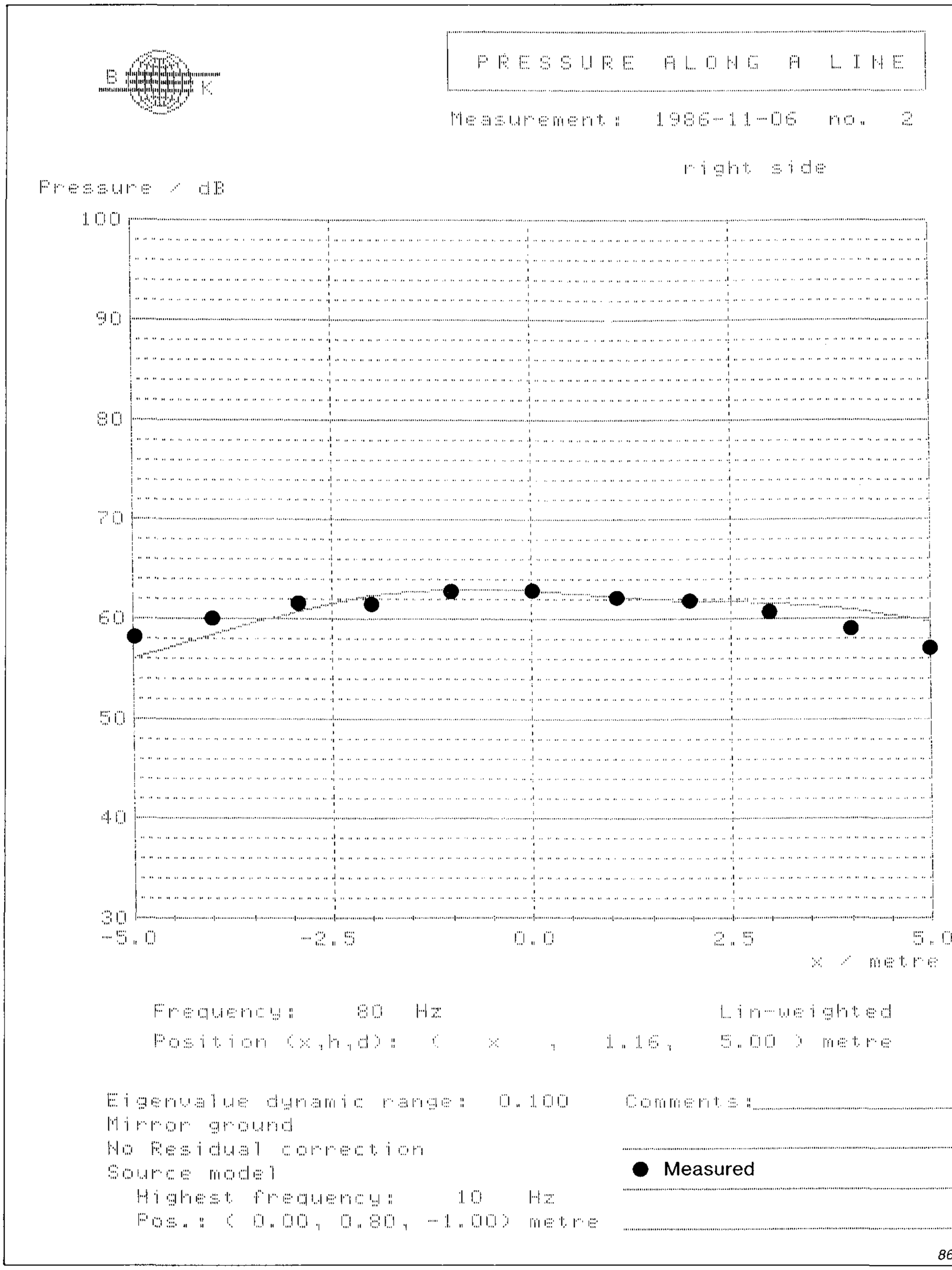

Fig. 15. Comparison between calculated and measured sound pressure level along a line. The source was a passenger car in a semi-anechoic chamber

4.3. Measurement of tyre noise

The tyres under test were mounted on a car which was run in free gear on a dynamometer. The surface of the rotating road was gravelled and the simulated speed was 60 km/hr. The measurements were performed using the narrowband STSF system Type 9606. The scan plane was 7 cm from the wheel. Twelve microphones were scanned over 20 positions. Three reference microphones were used. The total measurement time was less than 30 minutes. The results were stored in the form of synthesized 100 Hz bands. Figs. 16 and 17 show the active and reactive intensity distribution at the surface of the wheel for the 100 Hz band centred at 400 Hz. The phenomenon of circulating acoustical energy can be seen in the active intensity plot. The main noise sources are in the vicinity of the tyre/roller contact area.

At the higher frequency of 2000 Hz, the active intensity plot shows how virtually all noise generation is related to the tyre/roller contact area (Fig. 18). The reactive intensity plot (Fig. 19) suggests that there is a periodic series of pressure maxima around the rim of the tyre perhaps associ-

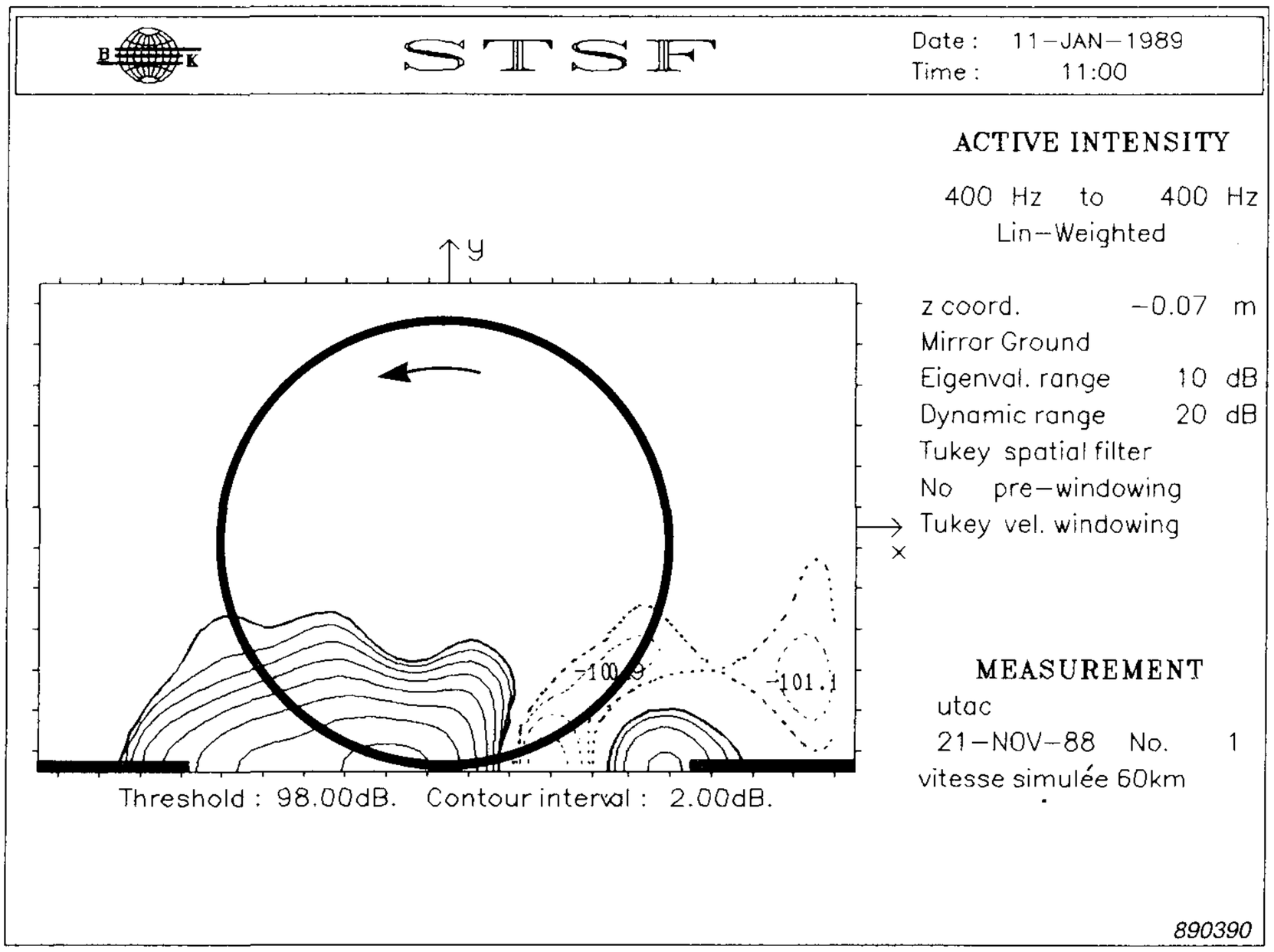

Fig. 16. Active intensity at the wheel surface ($z = -0{,}07$ m) at 400 Hz. The dotted curves indicate regions of negative intensity

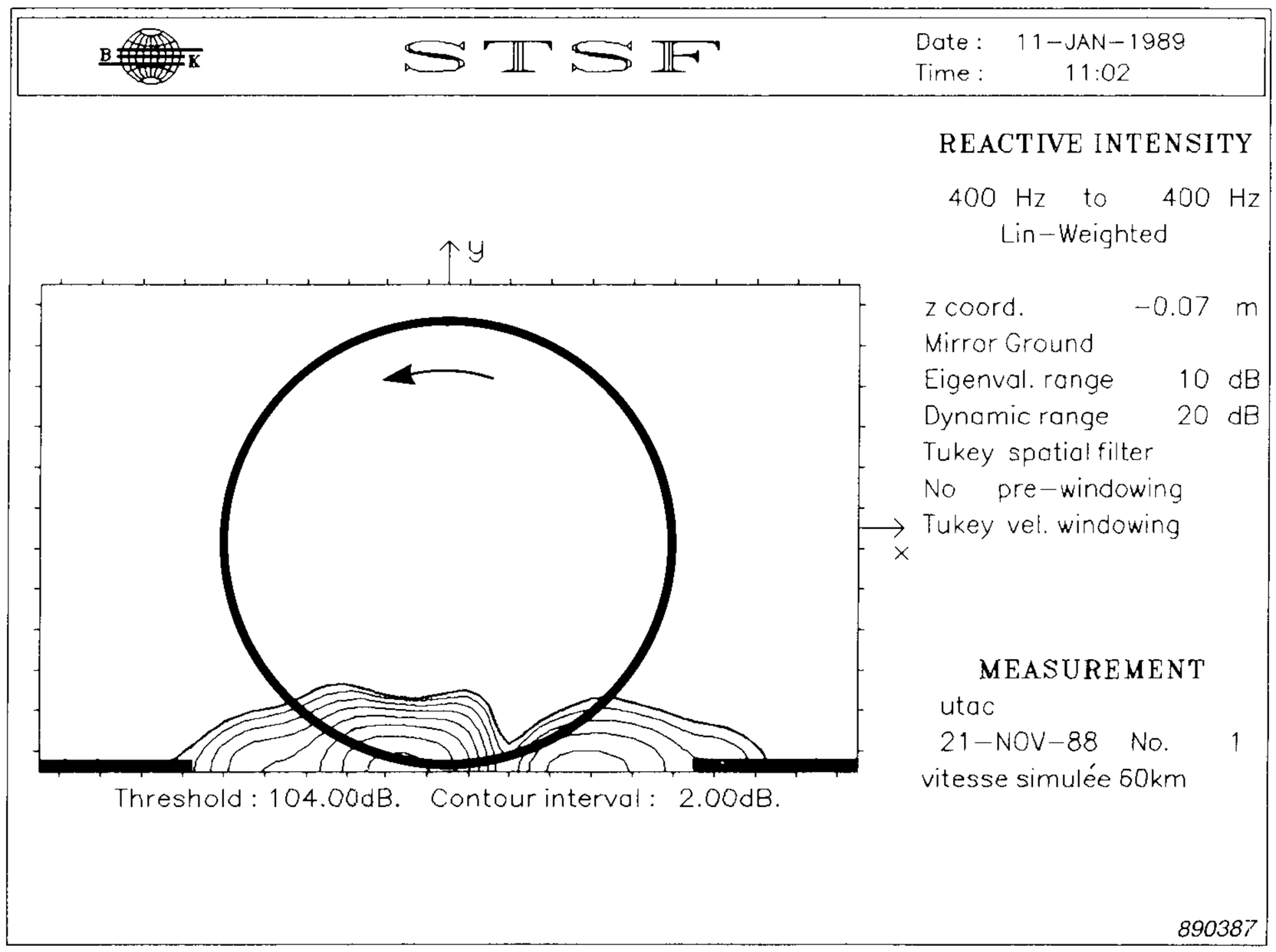

Fig. 17. Reactive intensity at the wheel surface ($z = -0{,}07$ m) at 400 Hz

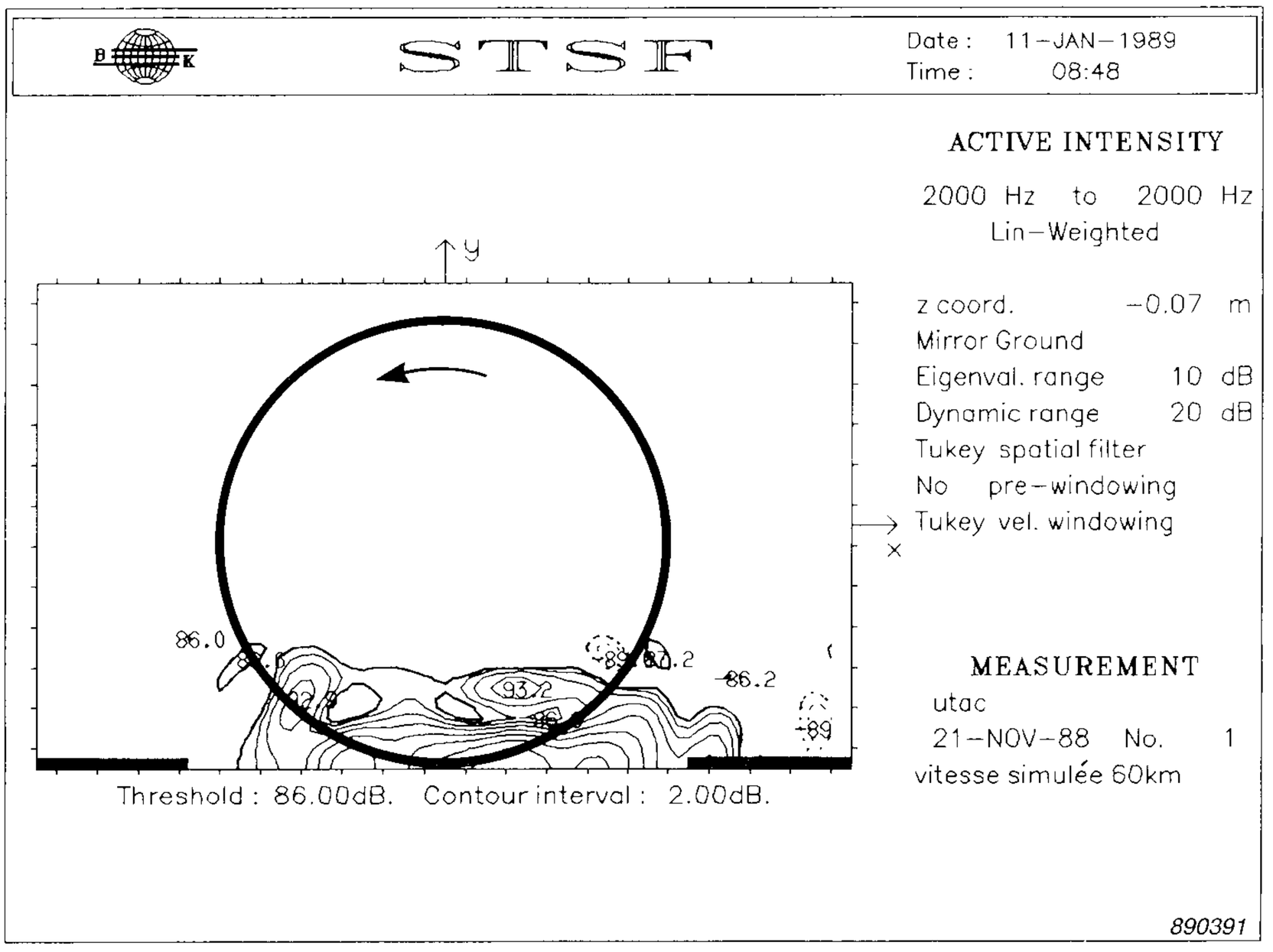

Fig. 18. Active intensity at the wheel surface ($z = -0{,}07$ m) at 2000 Hz

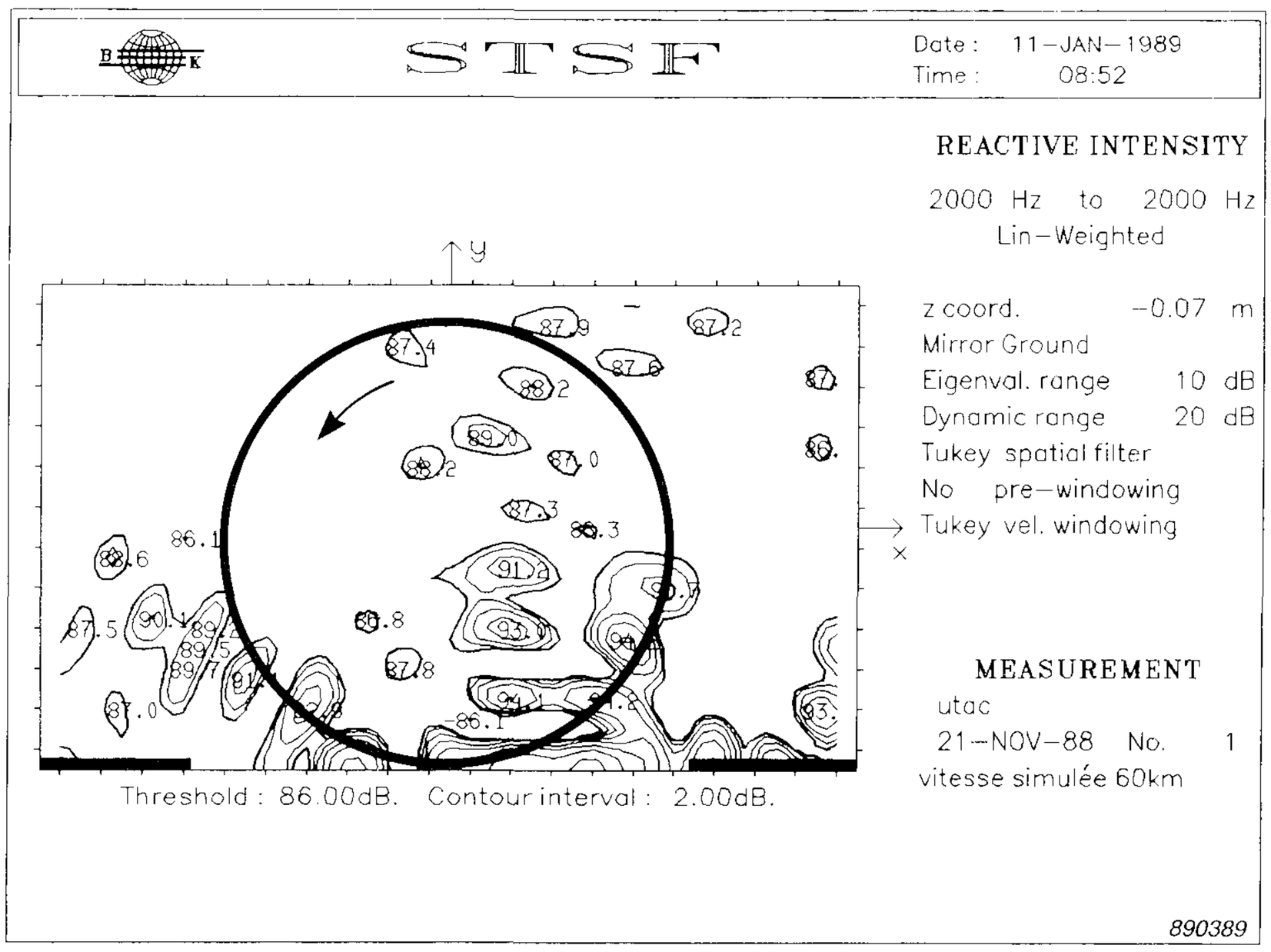

Fig. 19. Reactive intensity at the wheel surface (z = −0,07 m) at 2000 Hz

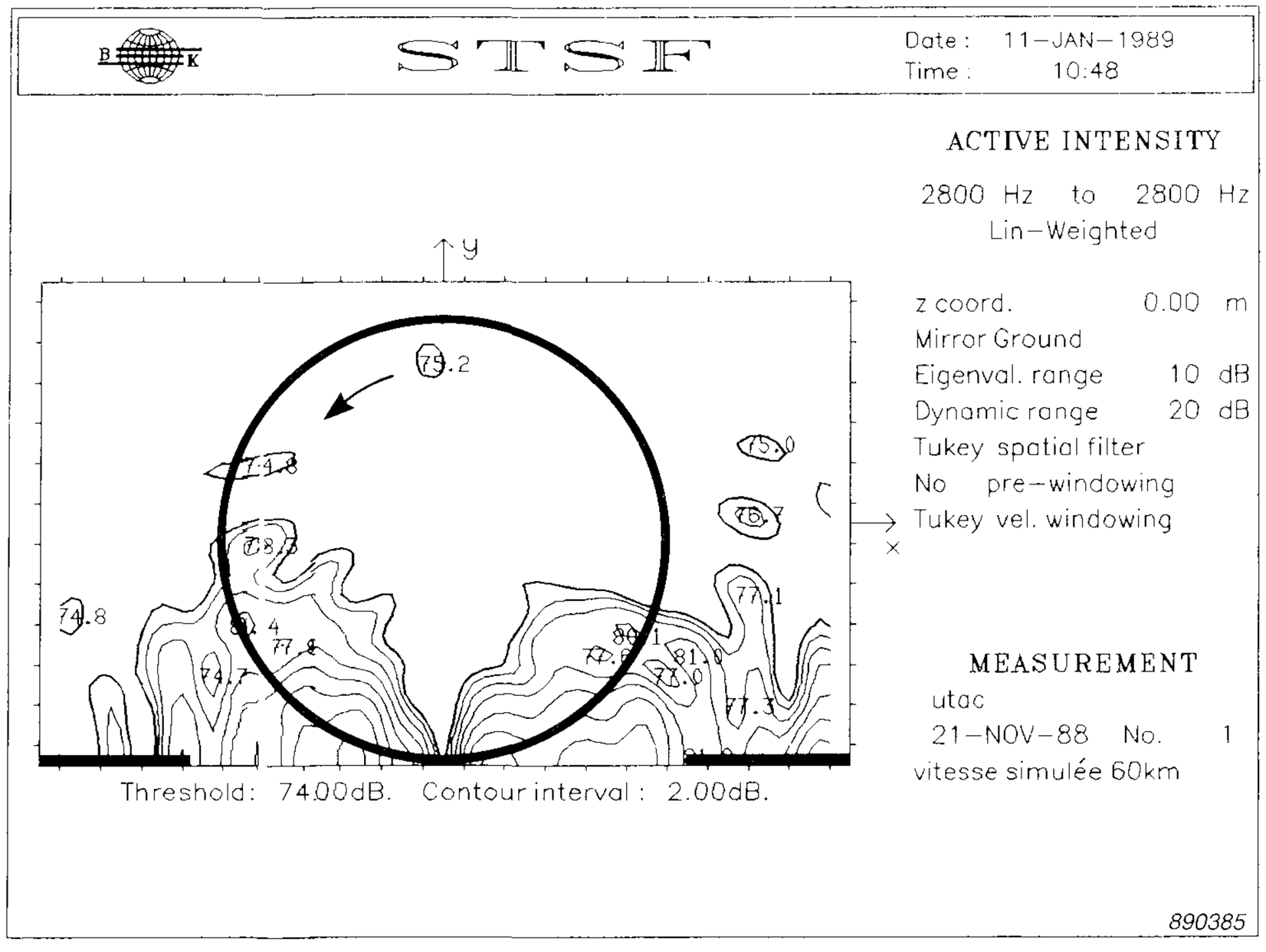

Fig. 20. Active intensity in the scan plane (z = 0,0 m) at 2800 Hz

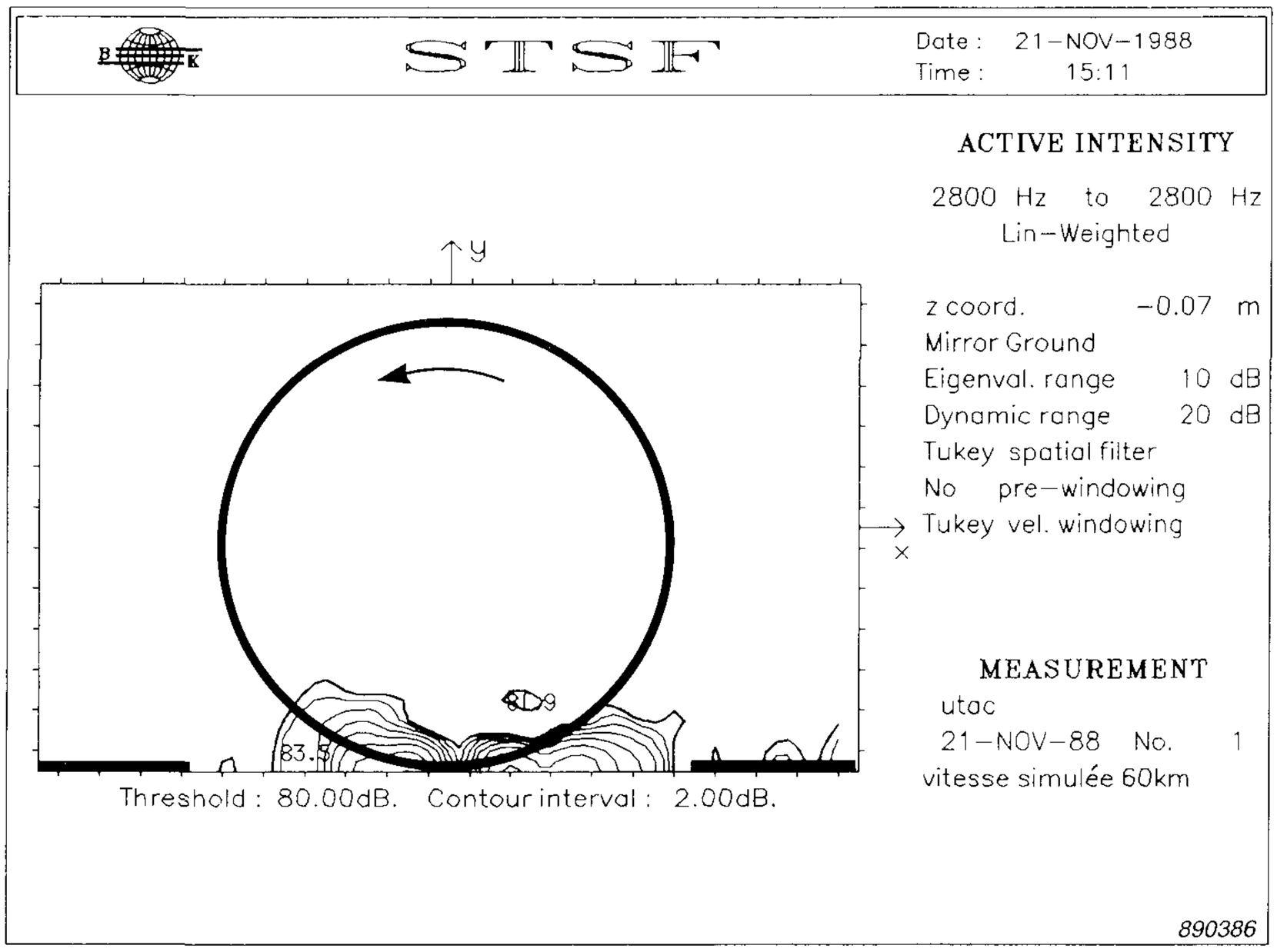

Fig. 21. Active intensity at the wheel surface (z = −0,07 m) at 2800 Hz

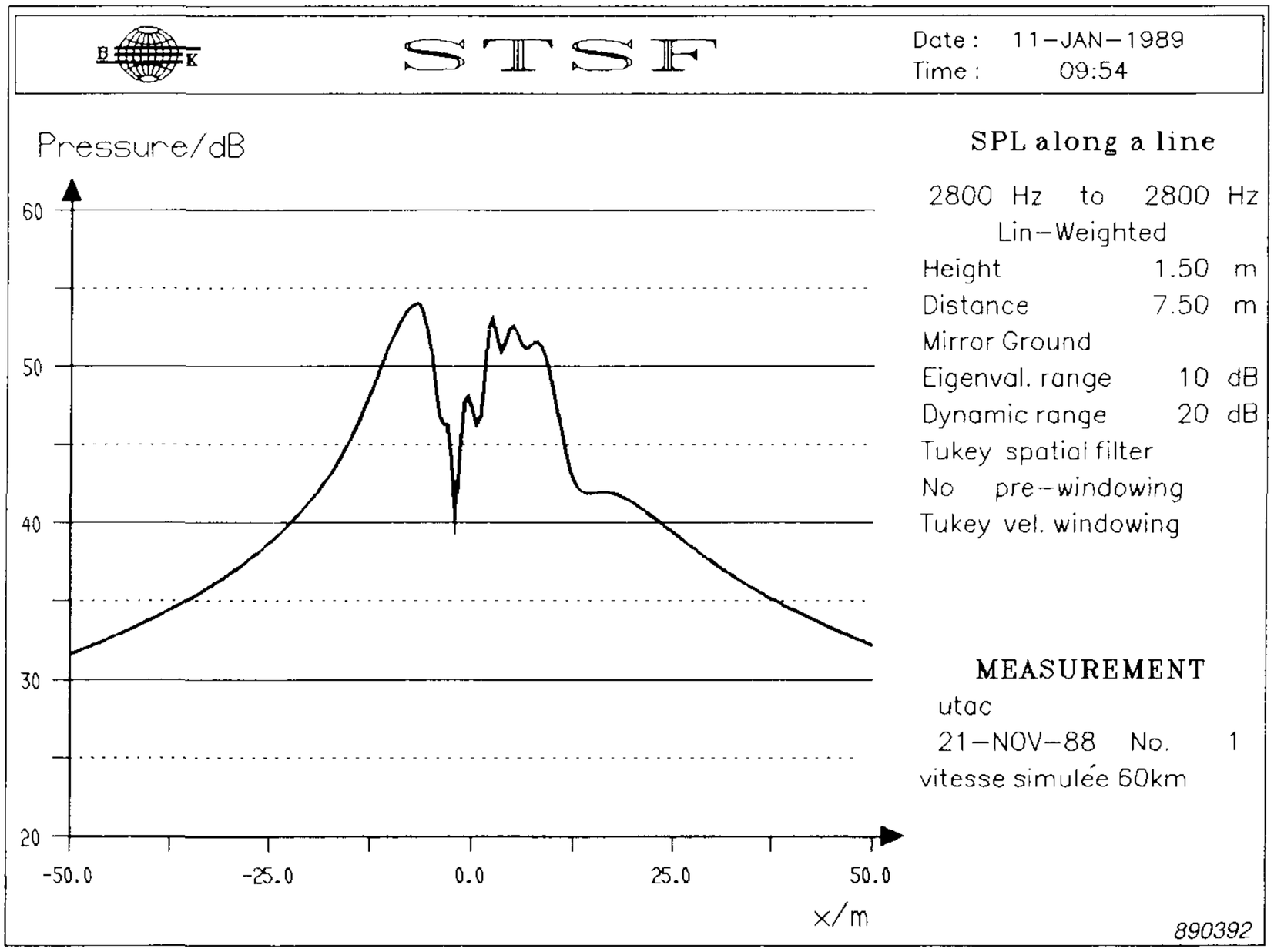

Fig. 22. Pressure along a line at 7,5 m from the car at 2800 Hz. Scale along x axis ± 50 m

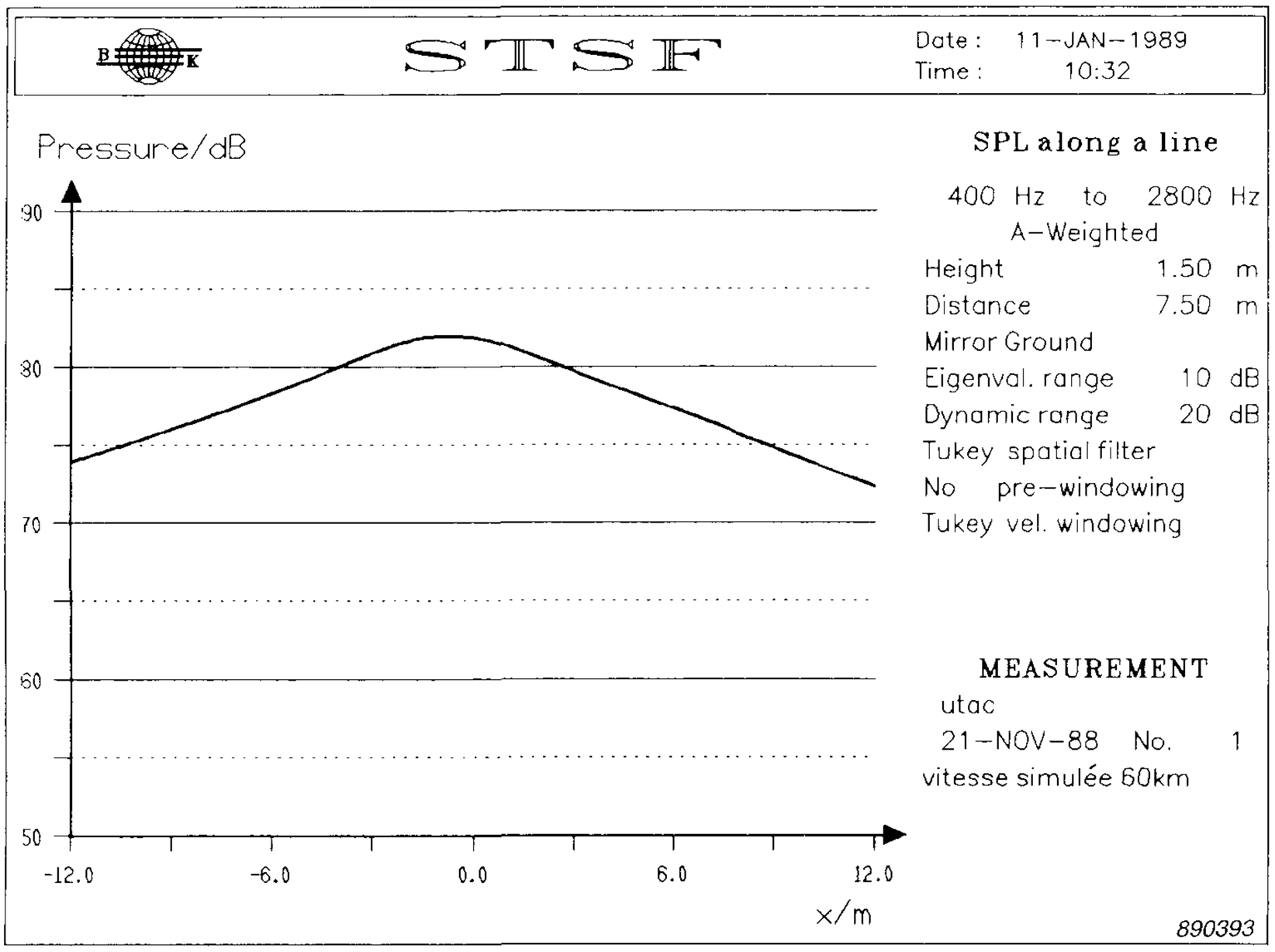

Fig. 23. The overall A-weighted sound pressure level in the frequency range 400 Hz to 2800 Hz at 7,5 m from the car

ated with the tyre's vibration. The 2800 Hz active intensity plot clearly shows the presence of two equally large sources (Fig. 20). Translation of the data in Fig. 20 to the surface of the wheel (Fig. 21) shows how the active intensity plot is focussed. Fig. 22 is the calculated sound pressure level along a line situated at 7,5 m from the car, at 1,5 m above a reflecting ground in the 100 Hz band centred around 2800 Hz. Notice the very sharp minimum on axis which is due to the dipole effect. The line length has been chosen to be from −50 m to + 50 m for the sake of clarity. The calculation is most accurate in the region around the axis i.e. ± 45° corresponding in this case to ± 7,5 m. The overall sound pressure level at 7,5 m from the car in the A-weighted frequency range from 400 Hz to 2800 Hz is shown in Fig. 23.

4.4. Measurements on a work station

Two STSF measurements were performed over the front of a free standing workstation (0,15 × 0,6 × 0,8 m) at a distance of 7 cm using firstly two reference microphones and secondly one reference accelerometer. The refer-

ence microphones were positioned close to the noise sources of interest: the fan and the disc drive. The accelerometer was fastened with wax directly to the disc drive's casing. Figs. 24 to 26 show three active intensity plots obtained from the measurement using reference microphones. Fig. 24 shows the total field. Figs. 25 and 26 show the partial fields no. 1 and no. 2 respectively. It should be noted that the term partial field as used here means in fact virtual partial field i.e. a linear combination of the actual partial fields. These calculated partial fields correspond well with the position of the disc drive and the ventilation grills and other openings in the cabinet. Fig. 27 was obtained from the measurement which used a reference accelerometer. It represents the part of the total sound field which is coherent with the vibration of the disc drive's casing. This part of the field is seen to be very similar to the partial field no. 1. Thus STSF can be used to assess the relative importance of the various partial fields on the total sound field. Alternatively a particular noise source can be "isolated" by placing an accelerometer directly on its surface. For delicate or lightweight structures a non-contact laser vibrometer could be used.

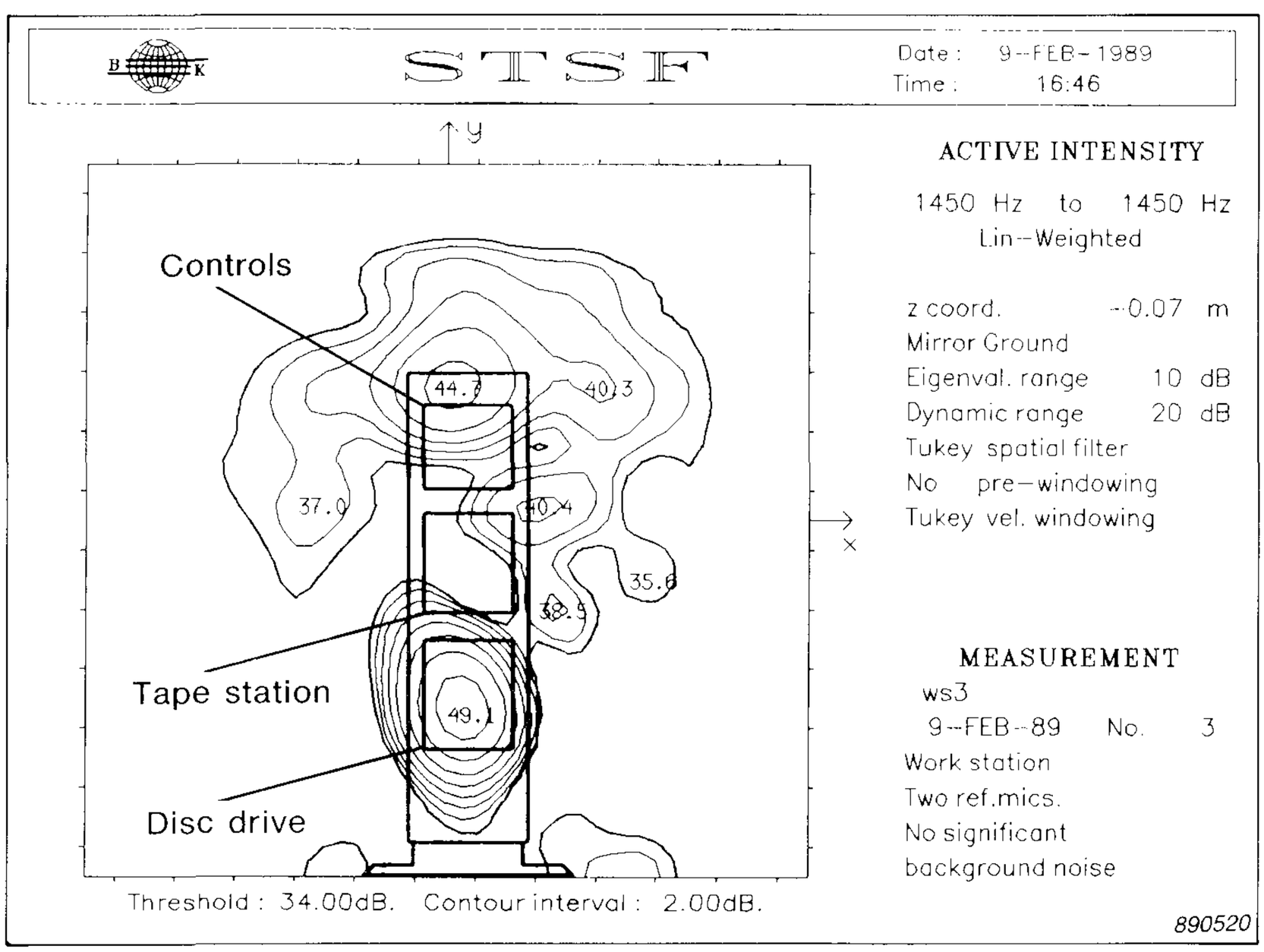

Fig. 24. Active intensity: 1450 Hz, total field, two reference microphones

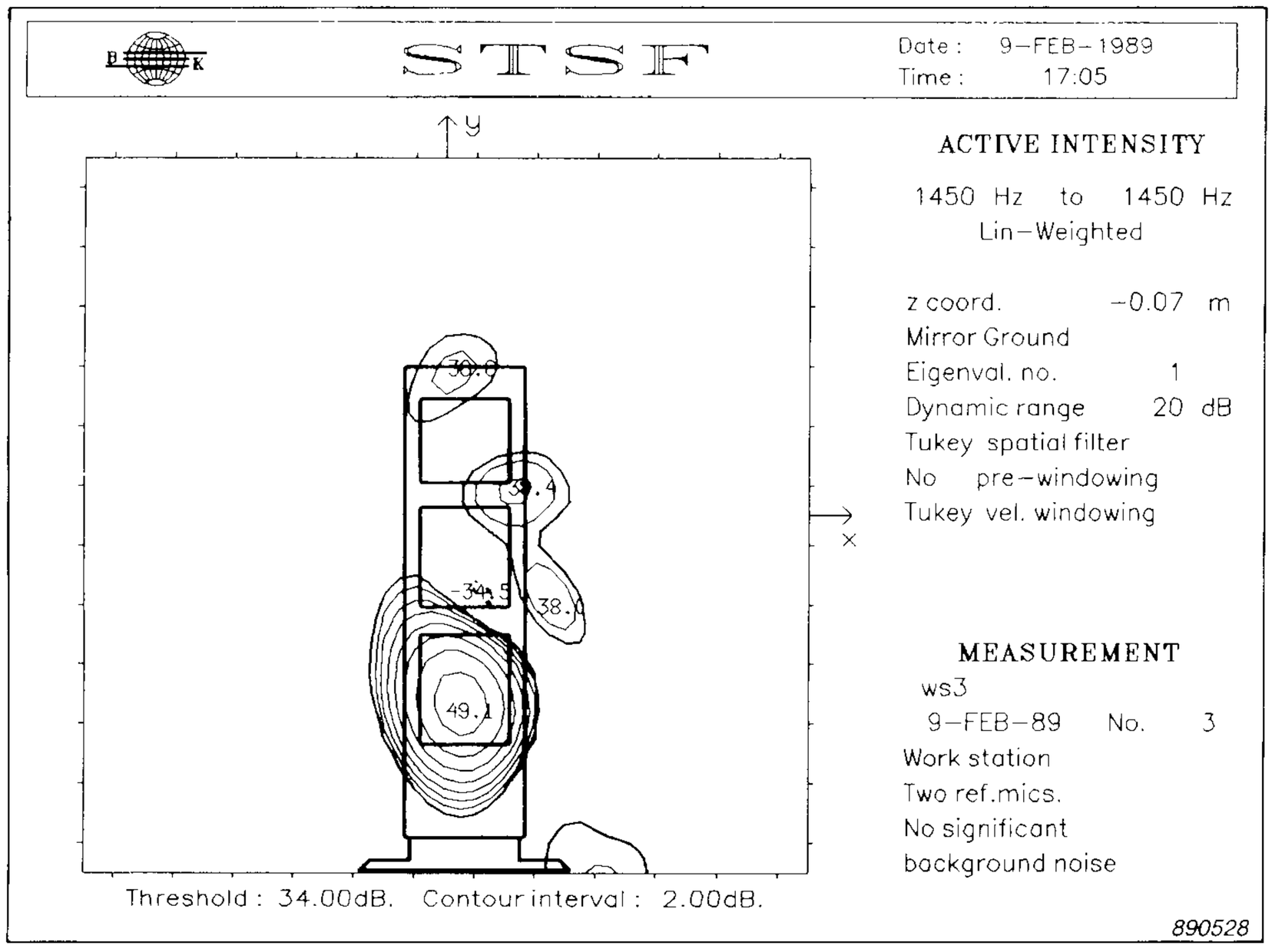

Fig. 25. Active intensity: 1450 Hz, partial field no.1, two reference microphones

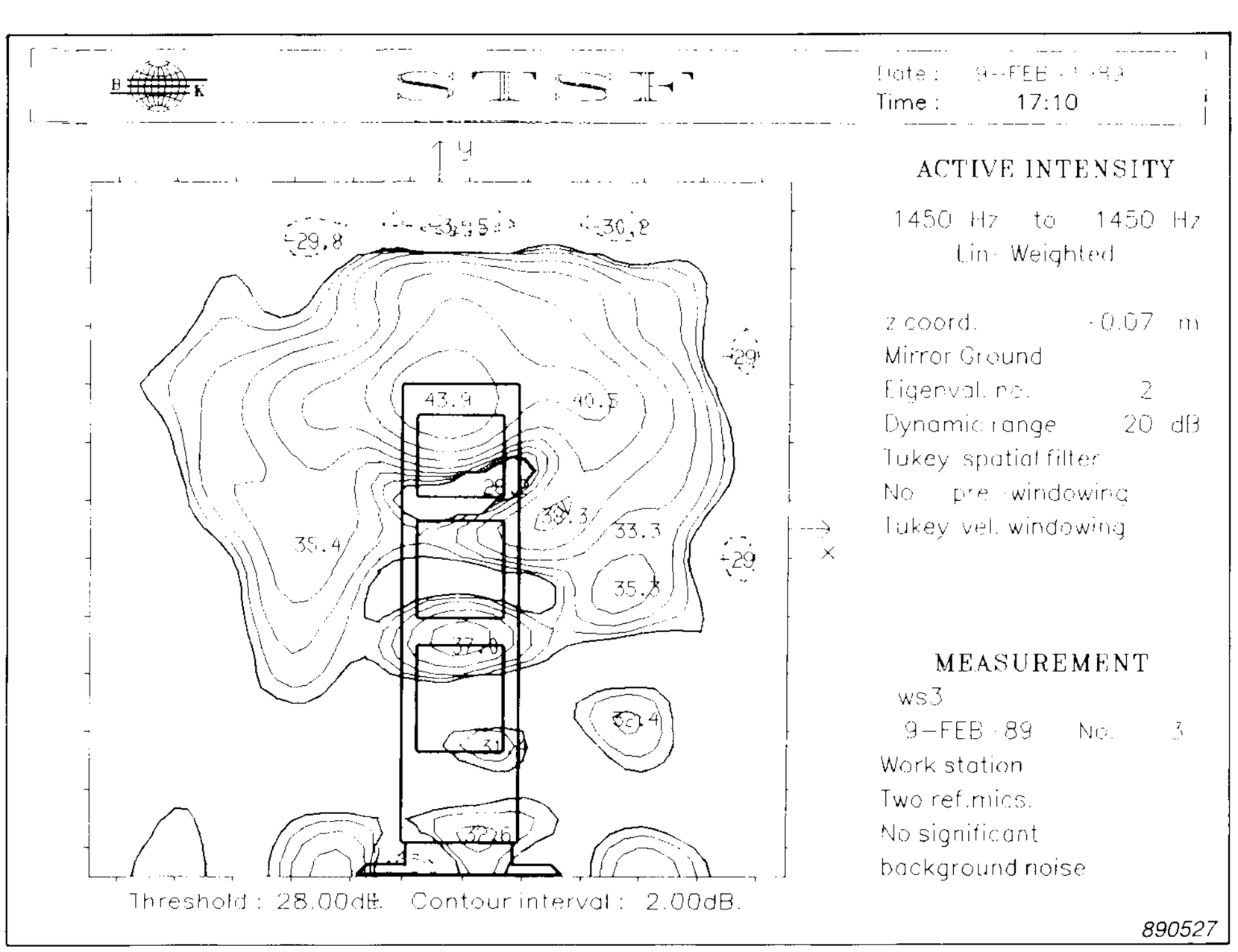

Fig. 26. Active intensity: 1450 Hz, partial field no.2, two reference microphones

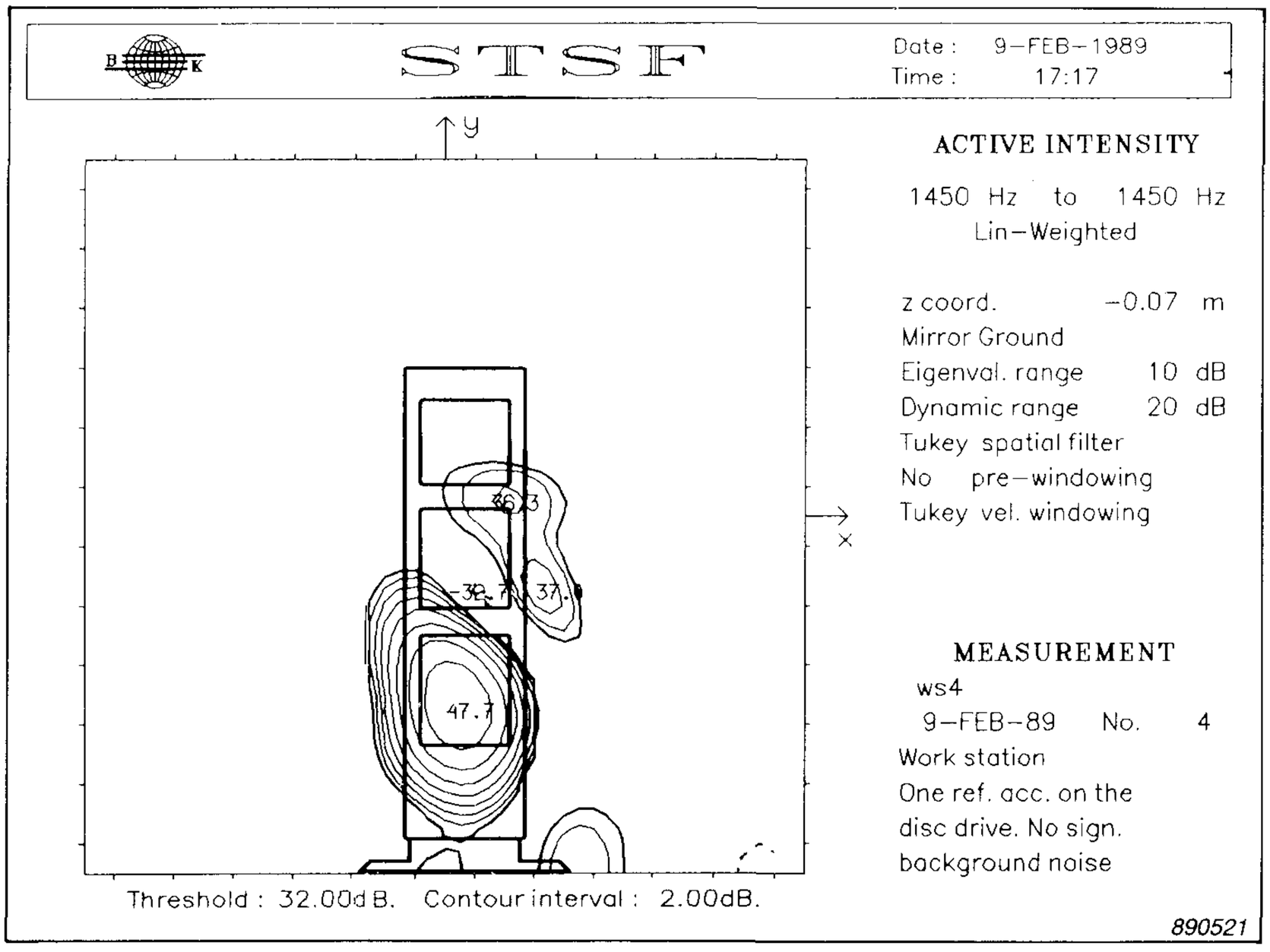

Fig. 27. Active intensity: 1450 Hz, total field, one reference accelerometer on the disc drive

Conclusions

The STSF technique employs an efficient principal component measurement technique to achieve a cross spectral representation of the sound field. Three practical instrumentation systems together with menu driven programs have been developed which enable the user to obtain a wealth of information about the noise fields under investigation. Examples of applications of the technique have been described to illustrate how STSF can be used by noise control engineers.

References

[1] Hald, J.: "*STSF–a unique technique for scan-based near-field acoustic holography without restrictions on coherence*", Technical Review No. 1, 1989, B & K publication

[2] Astrup, T.: "*Acoustic intensity and spatial transformation used to describe the sound field around a seismic vibrator*", Proceedings of Nordic Acoustic Meeting, 1986, pp.413–415

[3] Ginn, K.B. & Hald, J.: "*Source location using accelerometers as reference transducers for the STSF technique*", Proceedings of ICA, 1989

[4] Hald, J.: "*Development of STSF with emphasis on the influence of bandwidth; Part I, Background and Theory*", Noise Con. Proceedings, 1988

[5] Ginn, K.B. & Hald, J.: "*Development of STSF with emphasis on the influence of bandwidth; Part II, Instrumentation and computer simulation*", Noise Con. Proceedings, 1988

Digital Filter Analysis: Real-time and Non Real-time Performance

Svend Gade

Abstract

This article demonstrates how the upper frequency limit for a digital real-time filter analyzer can be extended without need for increased processing capacity or increased sampling frequency.

A consequence of this kind of signal processing is that some of the filters will be operating in non real-time in such measurement mode.

Sommaire

Cet article démontre comment la limite haute fréquence d'un analyseur en temps réel à filtrage numérique peut être améliorée sans recourir à l'augmentation des capacités de traitement ou de la fréquence d'échantillonnage.

L'inconvénient de ce type de traitement de signal est que quelques filtres ne fonctionnent plus en temps réel dans un tel mode de mesure.

Zussammenfassung

Die obere Frequenzgrenze eines Echtzeit-Analysators mit digitalen Filtern läßt sich erhöhen, ohne daß größere Verarbeitungskapazität oder höhere Abtastfrequenz nötig sind. Einige Filter arbeiten dann jedoch nicht in Echtzeit.

Introduction

In acoustics there is a long tradition for using 1/1 octave and 1/3 octave analysis i.e. constant percentage bandwidth analysis by means of analogue filters. The use of digital filters operating in real-time up to 20 kHz was introduced in the mid seventies Ref. [1]. The interest in having a more narrow yet relative frequency resolution has resulted in the introduction of a new generation of digital constant percentage bandwidth filter analyzers with the choice of 1/1, 1/3, 1/12 and 1/24 octave analysis, namely the Brüel & Kjær Real-time Frequency Analyzer Type 2123 and Dual Channel Real-time Frequency Analyzer Type 2133.

Using 1/12 octave and 1/24 octave analysis, the upper real-time frequency limit is restricted to respectively 4 kHz and 2 kHz (octave centre frequency in single channel mode) due to the requirement of calculation capacity in the signal processor. It will be shown how the upper frequency limit can be extended by two octaves at the cost of losing real-time capacity in the three highest octaves.

It should be noted that the signal processing described in this article *only* applies to analyzers without the High Frequency Expansion Unit, ZT 0318.

Digital Filters

Digital filters, which work on a sample to sample basis, consist of adders, multipliers and delay units Ref. [2]. The two-pole building blocks found in 2123 and 2133 (using software implementation as shown in Fig. 1), consist of two adders, two multipliers and two delay units.

Multiple-pole filters (generally required to achieve steep filter roll-off) can be formed by cascading two-pole sections. By appropriate choice of the coefficients (B_1 and B_2) it is possible to generate digital equivalents of all well-known filter types e.g. Butterworth, Chebyshev, etc. Ref. [3]. Thus these digital filters have an infinite impulse response (IIR–filters), which ensures consistency with data bases obtained using analogue filters.

One main advantage of a digital filter is that the same software (or hardware) can be used to generate any filter shape, e.g. 1/1 octave, 1/3 octave, 1/12 octave etc., just by changing the filter coefficients used in the calculations.

As shown later, digital filters are best adapted to logarithmic frequency scales and constant percentage bandwidth analysis, in contrast to DFT/FFT analysis which intrinsically yields constant bandwidth and is best presented on a linear frequency scale.

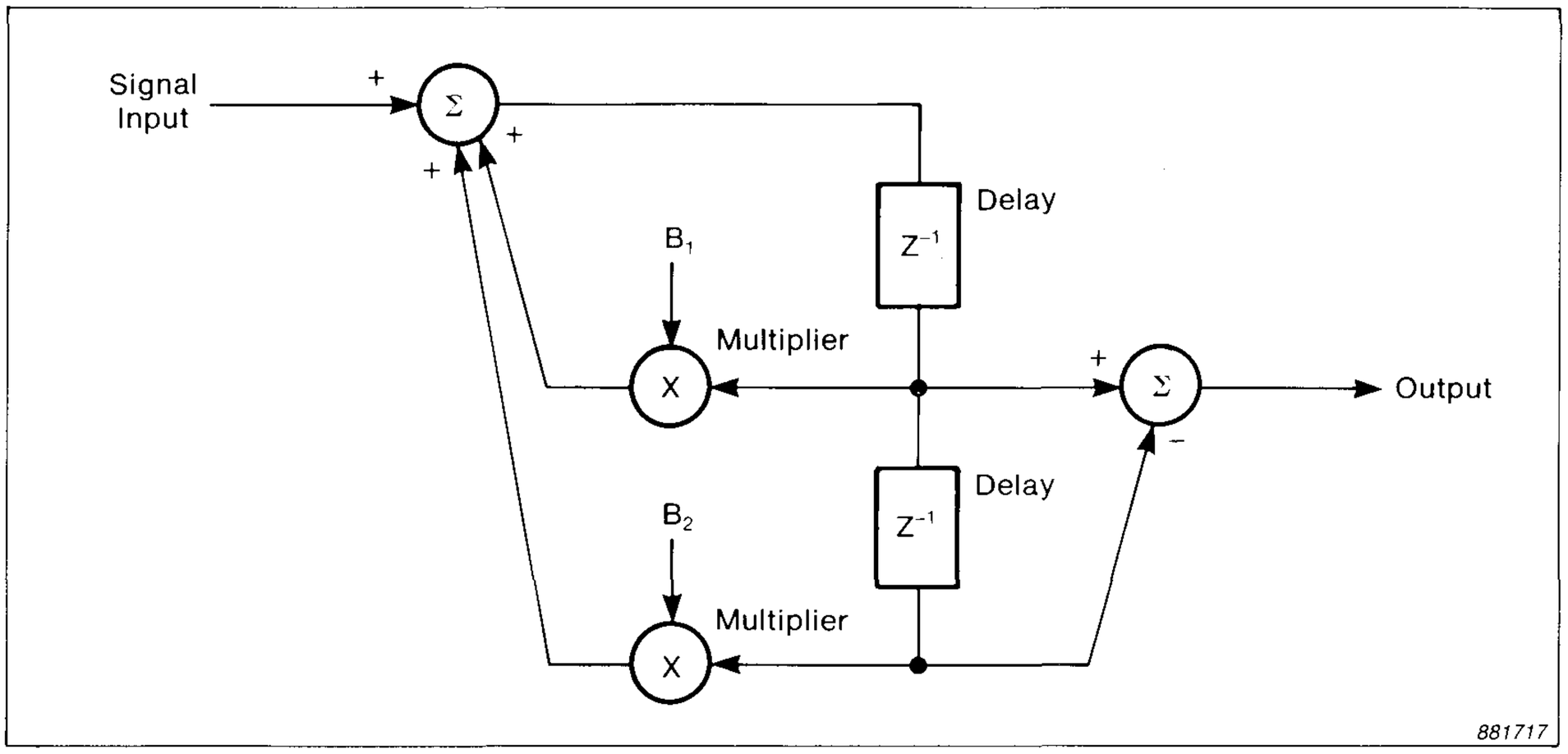

Fig. 1. Block Diagram of two-pole digital filter unit used in 2123 and 2133. Z^{-1} is a delay of one sampling period

Parallel Filtering

A parallel bank of 1/1 octave digital filters is obtained in the following manner:

Each sample coming from the ADC (Analogue to Digital Converter) is first bandpass filtered in the highest octave of interest and lowpass filtered (see Fig. 2).

The cut-off frequency of the lowpass filtering is one octave lower than the previous maximum frequency content. It is now possible to discard every second sample in the lowpass filtered signal without losing any further information, i.e. once the highest octave in frequency is filtered away it is quite valid to use half the previous sample rate while still complying with Shannon's Sampling Theorem†.

These lowpass filtered samples with half the sampling frequency can now be fed back to the bandpass filter section, and since – for all digital signal analysis – the filter characteristics are defined only in relation to the sampling frequency, the same filter coefficients will now give a new octave bandpass filter one octave lower in frequency.

† Shannon's Sampling Theorem states that a sampled time signal must not contain components at frequencies above half the sampling rate (the so-called Nyquist frequency)

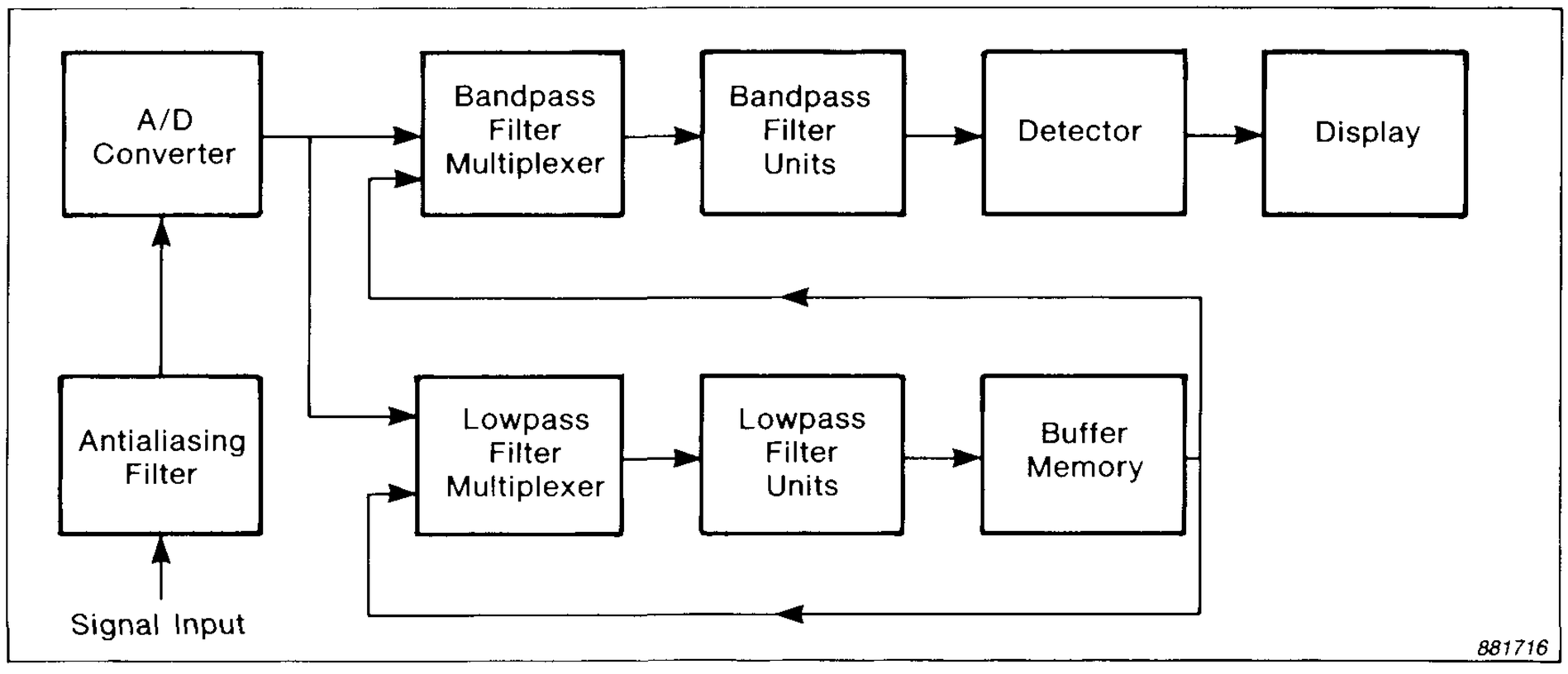

Fig. 2. Simplified Block Diagram for a Digital Filter Analyzer

In a similar manner, the lowpass filtered samples can be fed back to the lowpass filter and again filtered one octave lower, once again allowing each second sample to be discarded, and so on. Hence, a filter with the same characteristics, but with a centre frequency one octave lower, is created by halving the sampling rate.

In 2123 and 2133 this process is continued 17 times covering 18 octaves with octave centre frequencies from 16 kHz down to 0,125 Hz.

Considering the number of samples to be processed in each octave and calling the number in 16 kHz octave M, the number in the 8 kHz octave is $M/2$, in the 4 kHz octave $M/4$, and so on. Thus the total number of samples to be processed in all octaves below the highest is $M\,(1/2 + 1/4 + 1/8.....) = M$, i.e. the same number of samples as in the highest octave.

Consequently it is only necessary for the bandpass filtering to process one data value from the highest octave plus one other in one of the lower octaves in each sampling period to achieve real-time parallel filtering.

This decimation principle yields constant percentage bandwidth analysis which is best presented on a logarithmic frequency scale. The filter coefficients are slightly changed between every second decimation to achieve Decade filters rather than Octave filters, as specified in international filter standards.

Octave filters show the same relative filter characteristics when we move either one octave up or down in frequency, while Decade filters show the same relative filter characteristics when we move either one decade up or down in frequency. This means for example, that the octave bandwidth filters in single channel mode have centre frequencies given by $10^{(3n/10)}$ where n is an integer between -3 and 14.

Real-time Analysis

Using a sampling frequency of 2^{16} Hz = 65536 Hz the sampling period is 15,3 μs.

To obtain 1/3 octave single channel real-time analysis up to 22,4 kHz (16 kHz octave centre frequency) six bandpass and two low pass filtrations within one sampling period must be performed (see Fig. 3).

Highest Octave				A lower Octave			
LP	BP 1	BP 2	BP 3	LP	BP 1	BP 2	BP 3

881718

Fig. 3. Six bandpass and two lowpass filters must be processed within one sampling period to obtain single channel real-time 1/3 octave analysis

All 1/3 octave, 1/12 octave and 1/24 octave bandpass filters are six-pole filters achieved by cascading three two-pole filter units. The 1/1 octave bandpass filters are 14-pole filters except for the dual-channel mode *with* 16 kHz upper frequency limit, in which case six-pole filters are used. The lowpass filters are ten-pole filters using five two-pole filter units in cascade. Since one mathematical operation in the signal processor (multiplication or summation) takes approximately 100 ns one six-pole bandpass filtration takes 1,2 μs and one five-pole lowpass filteration 2 μs (see Fig. 1). Thus, the filtering done in Fig. 3 takes about 11,2 μs, is well within the sampling period and therefore in real-time.

Except for the order of the filters, the real-time frequency also depends on the number of measurement channels and the number of filters per octave (i.e. bandwidth) as shown in Fig. 4.

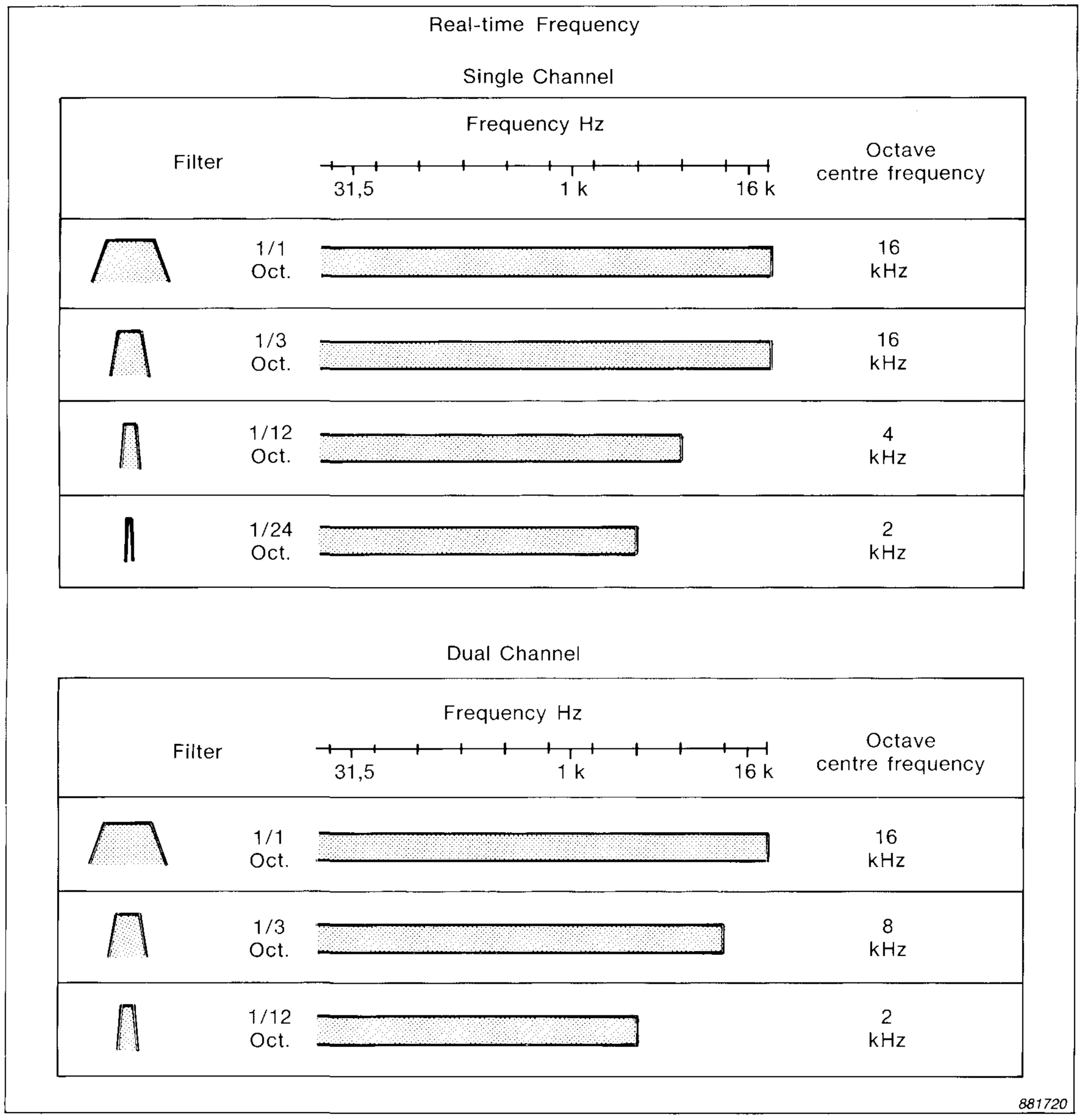

Fig. 4. Real-time frequency depends on the number of channels, the number of filters per octave (i.e. bandwidth) and the order of the filter

Frequency Extension in Non Real-time

For a single channel 1/12 octave analysis the real-time frequency limit is up to 4 kHz octave centre frequency. That is four times lower than for 1/3 octave analysis, because four times more filters have to be processed compared to 1/3 octave analysis. A maximum of six six-order bandpass filters including lowpass filtration can be calculated within one sampling period of 15,3 μs.

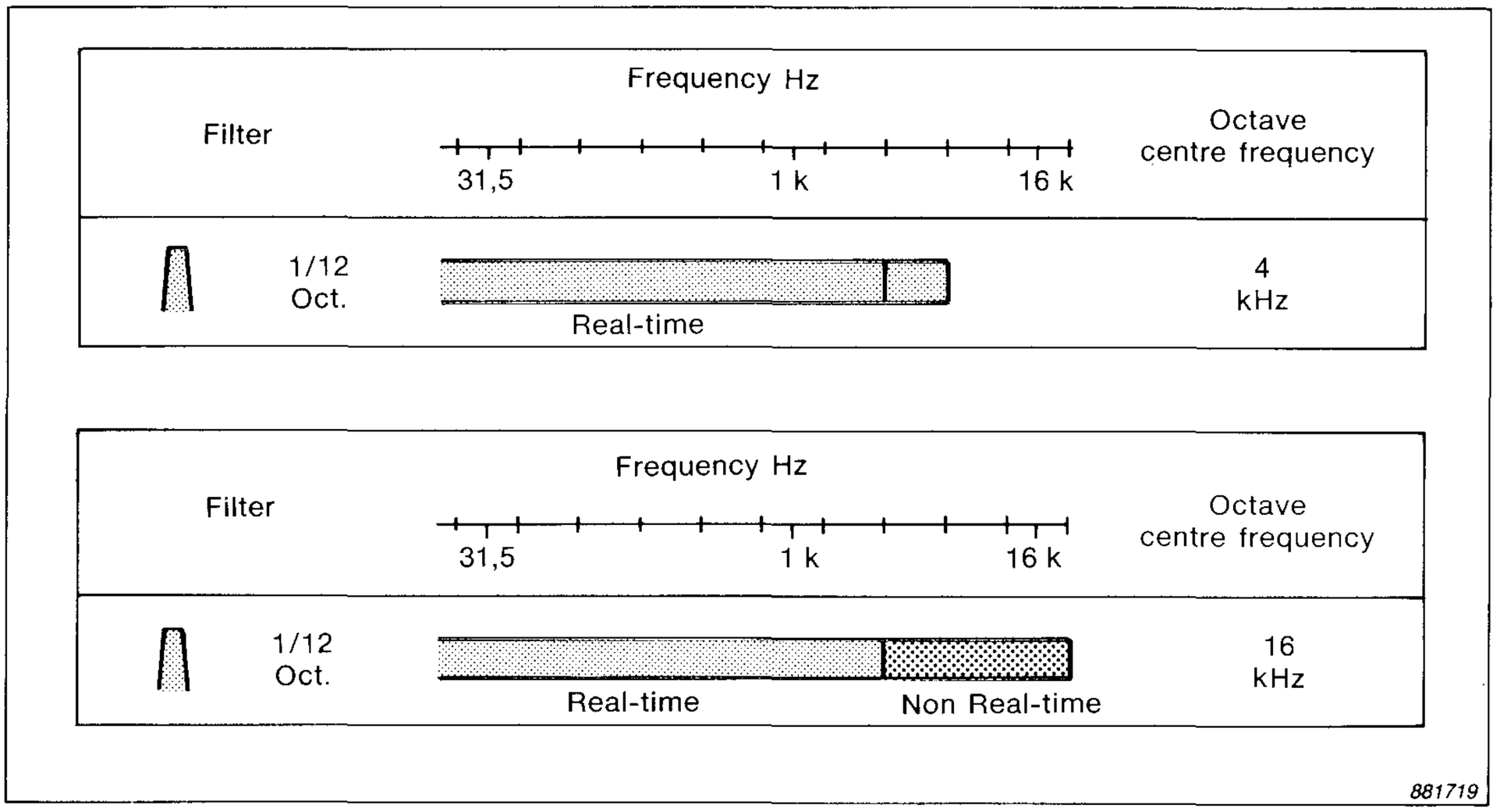

Fig. 5. Choice between real-time 1/12 octave analysis up to 4 kHz and partly non real-time analysis up to 16 kHz in single channel mode

Since 50% of the calculation time is used for processing the 12 filters in the 4 kHz octave in real-time, we could utilize this calculation capacity to process the filters in the three octaves 4 kHz, 8 kHz and 16 kHz but of course not in real-time.

This gives the choice between 1/12 octave analysis in real-time up to and including 4 kHz, or 1/12 octave analysis up to 16 kHz where the filters up to 2 kHz are processed in real-time, as shown in Fig. 5.

Non Real-time Filtering

In Fig. 6 it is shown for 1/12 octave single channel analysis how the 1/12 octave filters are working part-time for the three highest octaves in the signal processor. The figure shows in which octave and which partial octave group each individual sample will be processed. A partial octave group consists of three 1/12 octave filters in this case.

This "Parallel–Serial" processing means that the non real-time filtered octaves will not be updated simultaneously and with the same speed as the real-time filtered octaves. In Fig. 7 it is shown in which order the 36 non real-time 1/12 octave filters are updated in a cycle and displayed on the screen.

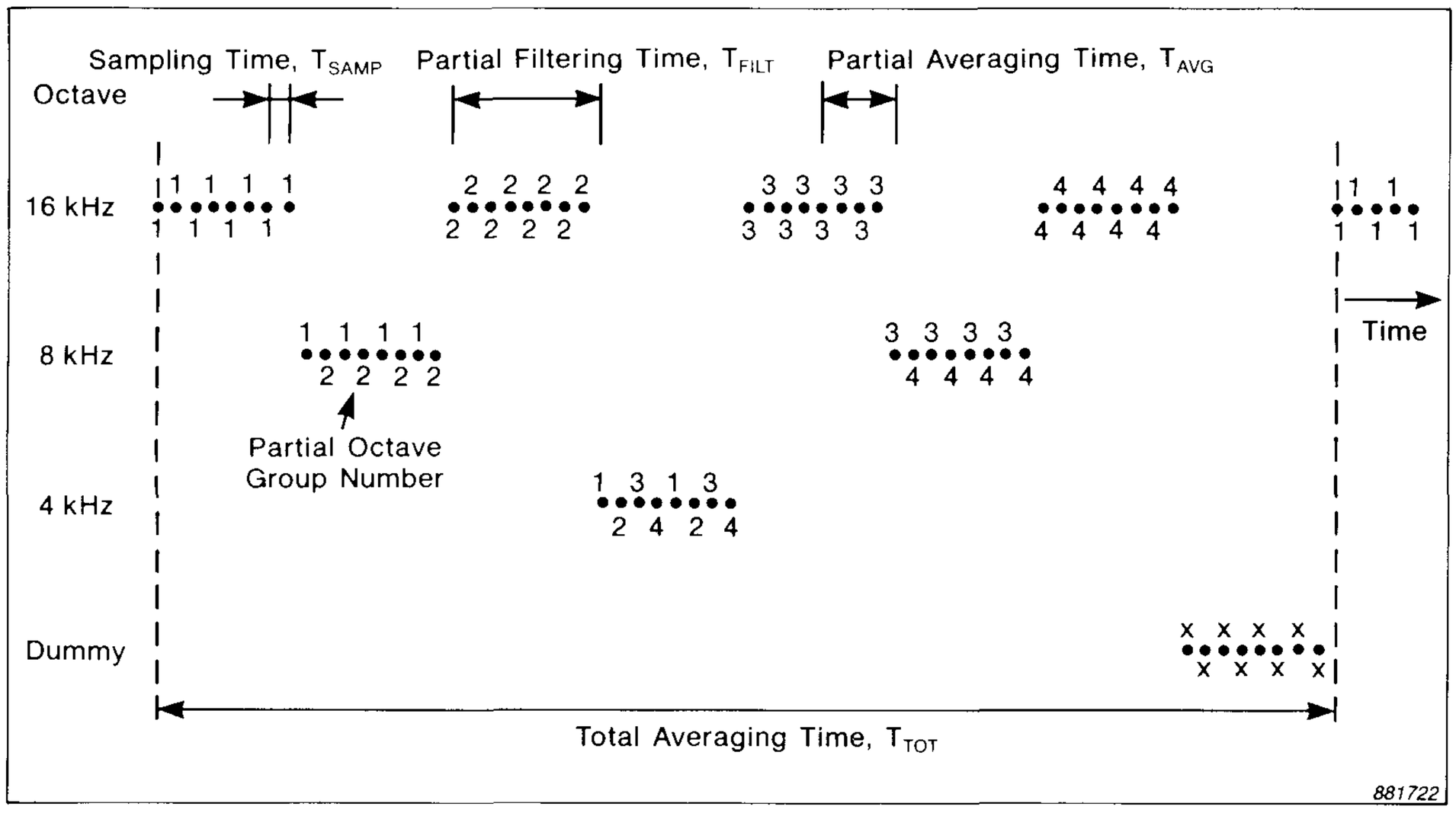

Fig. 6. Non real-time filtering in the signal processor. All samples are used except those for the dummy octave, which are discarded

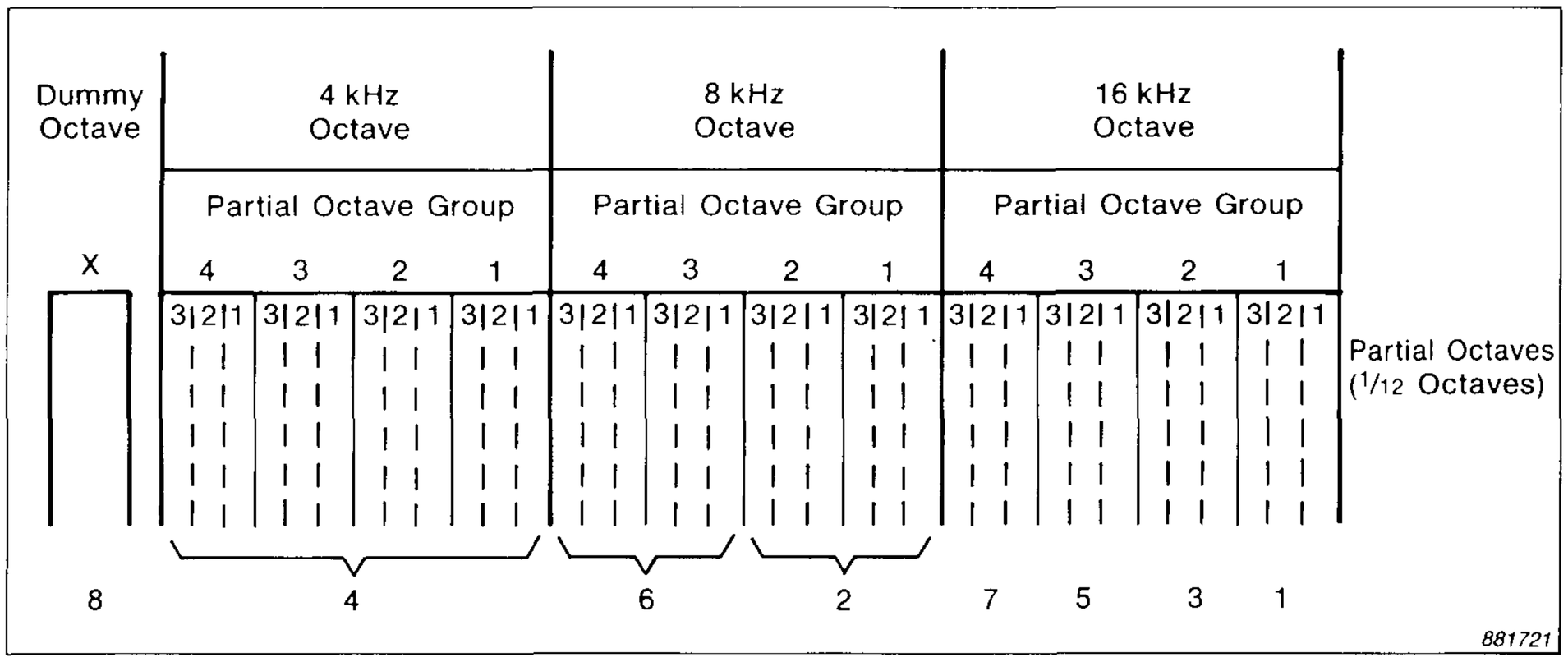

Fig. 7. The order at which the 1/12 octave filters are updated on the screen

First the three highest 1/12 octave filters in the 16 kHz octave are updated. Then the six highest filters in the 8 kHz octave are updated. The last filters updated in this sequence, except for the dummy octave, are the three lowest filters in the 16 kHz octave.

As can be seen from Fig. 6 the time the filters are active or working in a cycle, the *partial filtering time*, T_{FILT} is one eighth of the cycle time, T_{TOT}

$$T_{\mathrm{FILT}} = \frac{1}{8} \cdot T_{\mathrm{TOT}} \tag{1}$$

As will be shown later we also have a *partial averaging time*, T_{AVG} which is the effective time the signal from the filters is fed to the detector. This is one sixteenth of the cycle time.

$$T_{\mathrm{AVG}} = \frac{1}{16} \cdot T_{\mathrm{TOT}} \tag{2}$$

This means that if in the measurement setup a chosen *linear* averaging time, T_A is a multiple of the cycle time, then the effective averaging time in the highest three octaves is only 1/16 of the averaging time indicated in the measurement setup.

Thus the BT-product achieved in the 4 kHz, 8 kHz and 16 kHz octaves will be the same as for the 250 Hz, 500 Hz and 1 kHz octaves respectively.

For *exponential* averaging the achieved BT product will be in agreement with that in the measurement setup chosen averaging time, when the warning line beneath the non real-time filters has disappeared.

Partial Filtering Time

Non real-time filtering corresponds to applying a rectangular time window on the signal to be filtered. If this window is too short compared to the effective duration of the impulse response of the filter, this windowing will produce a smearing (leakage) of the frequency response of the filter. In other words, the filters have to "settle" before averaging can take place. Especially for very narrow filters a long *partial filtering time*, T_{FILT} is required.

Fig. 8 shows a typical impulse response function of a filter. From this picture it seems reasonable to choose a *partial filtering time* which is at least four to six times longer than the rise time, T_R of the filter. It is also shown that the rise time is approximately equal to the reciprocal of the filter bandwidth, B.

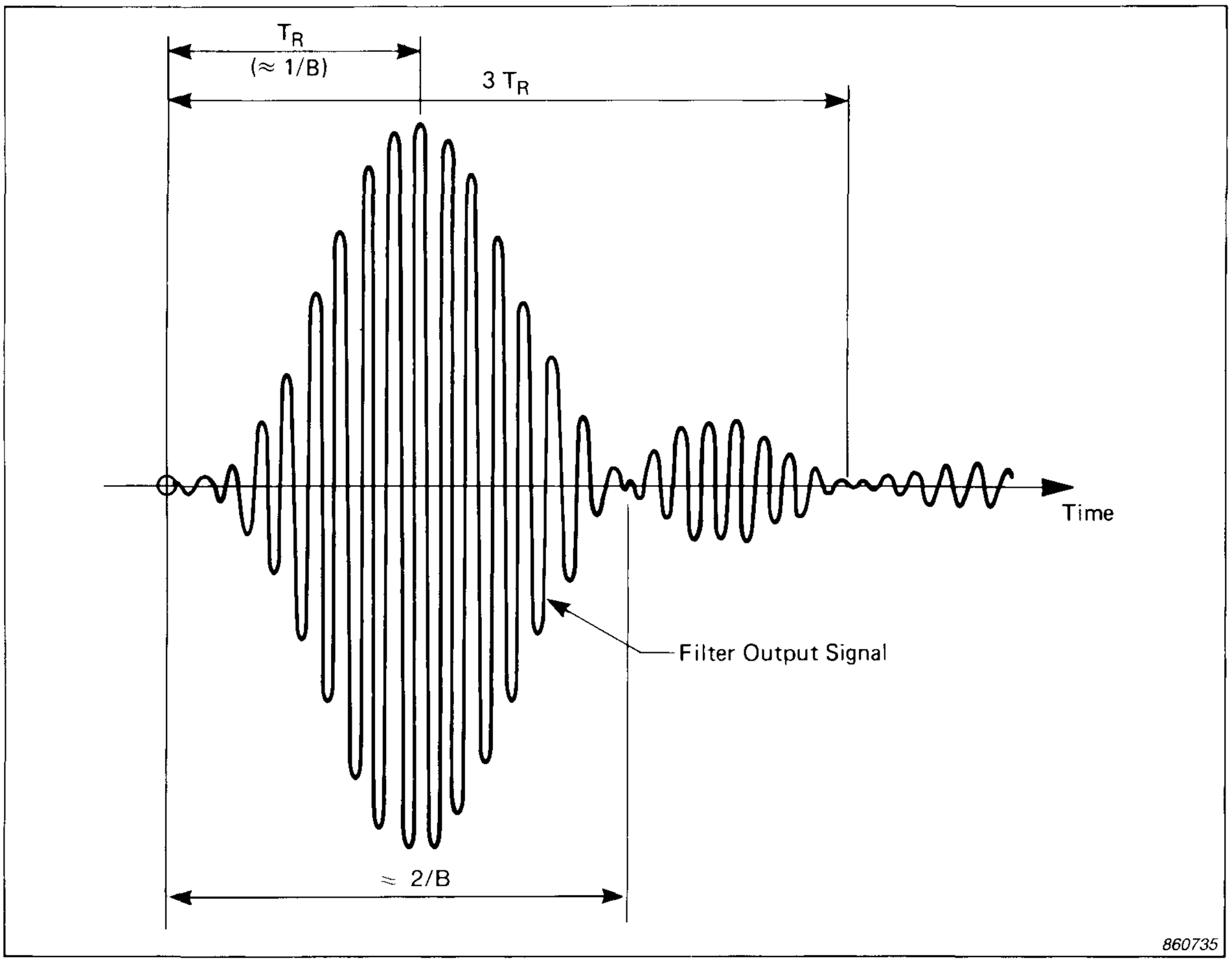

Fig. 8. Typical filter impulse response, where T_R is the filter rise time and B is the filter bandwidth

The largest effect of the windowing is found on the partial octave filter with the lowest centre frequency i.e. for single channel 1/12 octave analysis a filter with a centre frequency of f_c = 2900 Hz.

Thus for this filter we have

$$B = f_c \cdot \left(2^{1/24} - 2^{-1/24} \right) \approx 166 \text{ Hz} \tag{3}$$

$$T_r \approx \frac{1}{B} \approx 6 \text{ ms} \tag{4}$$

and a *partial filtering time* required is at least somewhat longer than 24 – 35 ms.

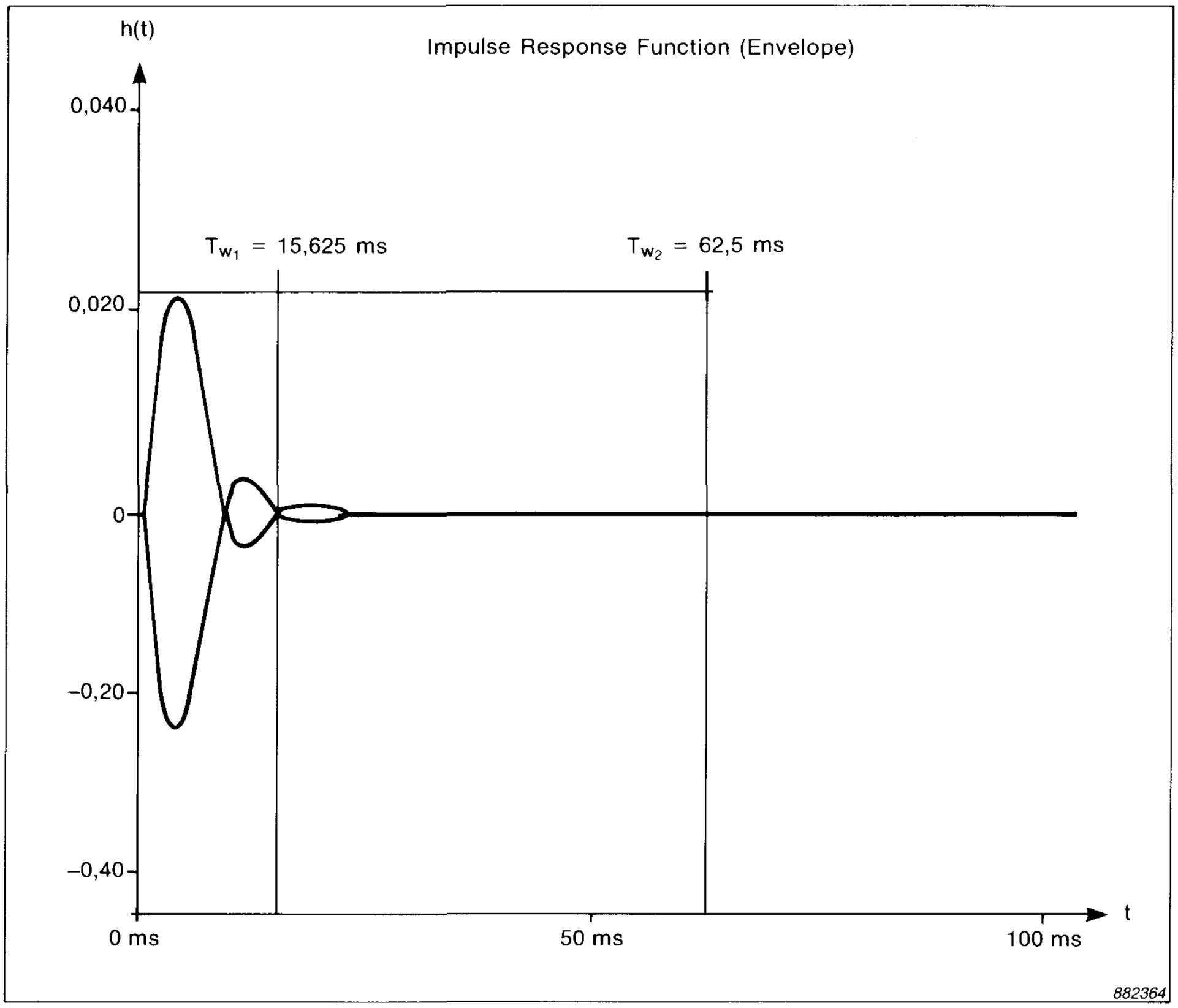

Fig. 9. Envelope of impulse response for the 1/12 octave filter with a centre frequency of 2900 Hz. Two rectangular windows with a length of 15,625 ms and 62,5 ms are shown

In Fig. 9 two examples of rectangular windows are shown on the envelope of the impulse response of the 1/12 octave filter with a centre frequency of 2900 Hz.

In the first example a window length of 15,625 ms corresponding to 256 data samples is used (the apparent sampling frequency is $f_s = 2^{14}$ Hz = 16384 Hz for the 4 kHz octave).

Fig. 10 shows how the envelope of the filter characteristic of the rectangular window is much broader than the filter characteristic of the 1/12 octave filter. Thus the resulting filter characteristics will be highly affected and mainly determined by the rectangular window.

In the second example found in Fig. 9, a window length of 62,50 ms corresponding to 1024 data samples is used.

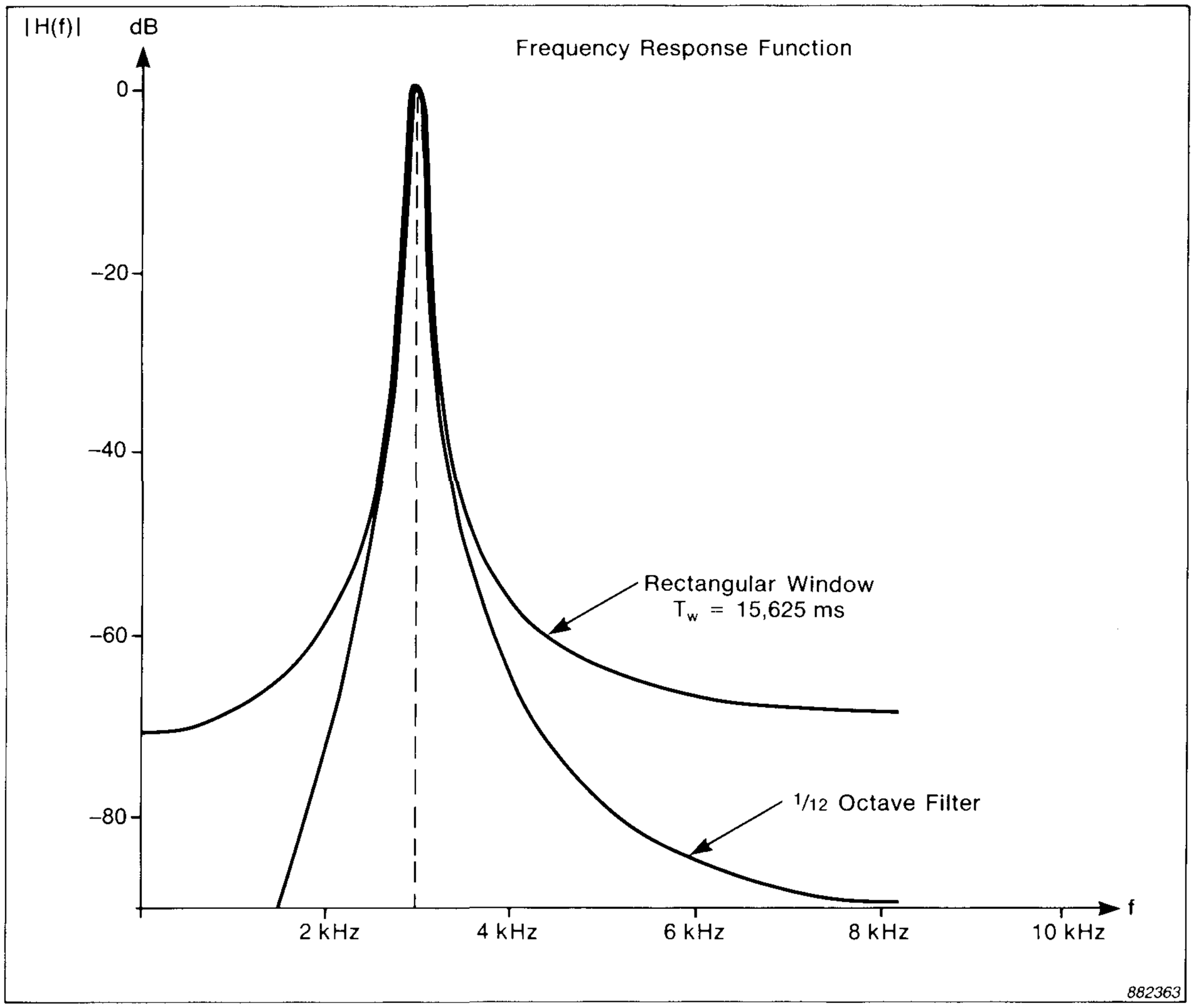

Fig. 10. Frequency response of the 1/12 octave filter with a centre frequency of 2900 Hz and the envelope of the frequency response of a rectangular window with a duration of 15,625 ms

Fig. 11 shows the overall filter characteristics, which in this case are identical to the filter characteristics of the 1/12 octave filter alone as shown in Fig. 10. Clearly, the windowing in the second example produces no smearing effect. Thus 62,50 ms is a proper choice of *partial filtering time* for the filter to be able to settle before an averaging of the output from the filter can take place.

For dual channel 1/12 octave analysis, the lowest non real-time octave band when using the non real-time frequency extension is 2 kHz. This means that the required *partial filtering time* for the filters to settle in this measurement mode is *twice* the *partial filtering time* for single channel operation, namely 125 ms.

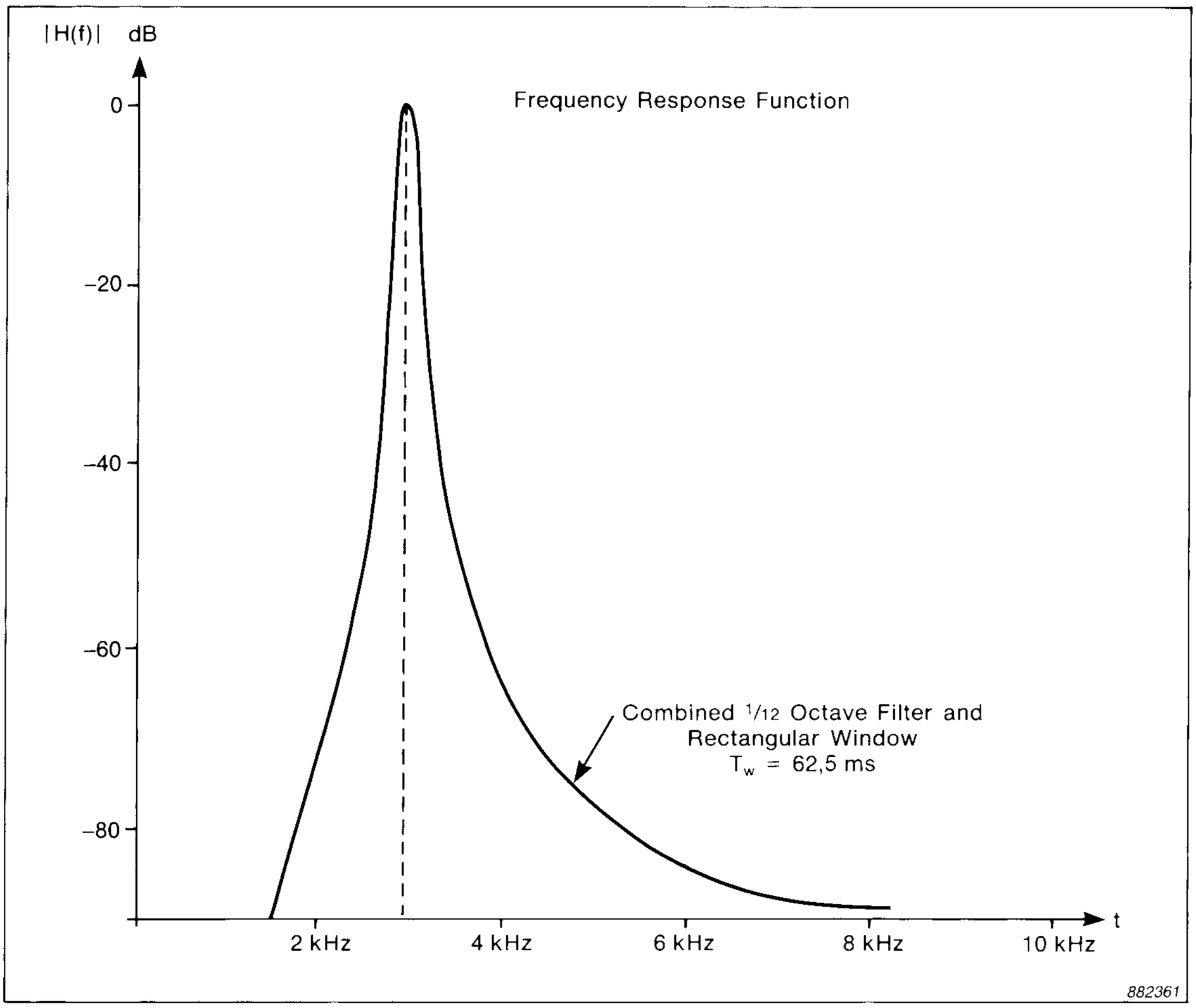

Fig. 11. Overall frequency response of the 1/12 octave filter with a centre frequency of 2900 Hz using a partial filtering time of 62,5 ms

Consequently for single channel 1/24 octave analysis the required *partial filtering time* will be 250 ms. To avoid making the total averaging time, T_{TOT} (see Fig. 6) or the cycle time (the interval between each screen update) too long, a *partial filtering time* of 125 ms for the 1/24 octave single channel analysis has been chosen. As a consequence a minor smearing effect of the filter characteristics, below –70 dB is found for this measurement mode, see Fig. 12.

Partial Averaging Time

The process of part time averaging also corresponds to applying a time window on the signal. The signal in this case is the squared output from the filters. The shortest possible *partial averaging time* in the signal pro-

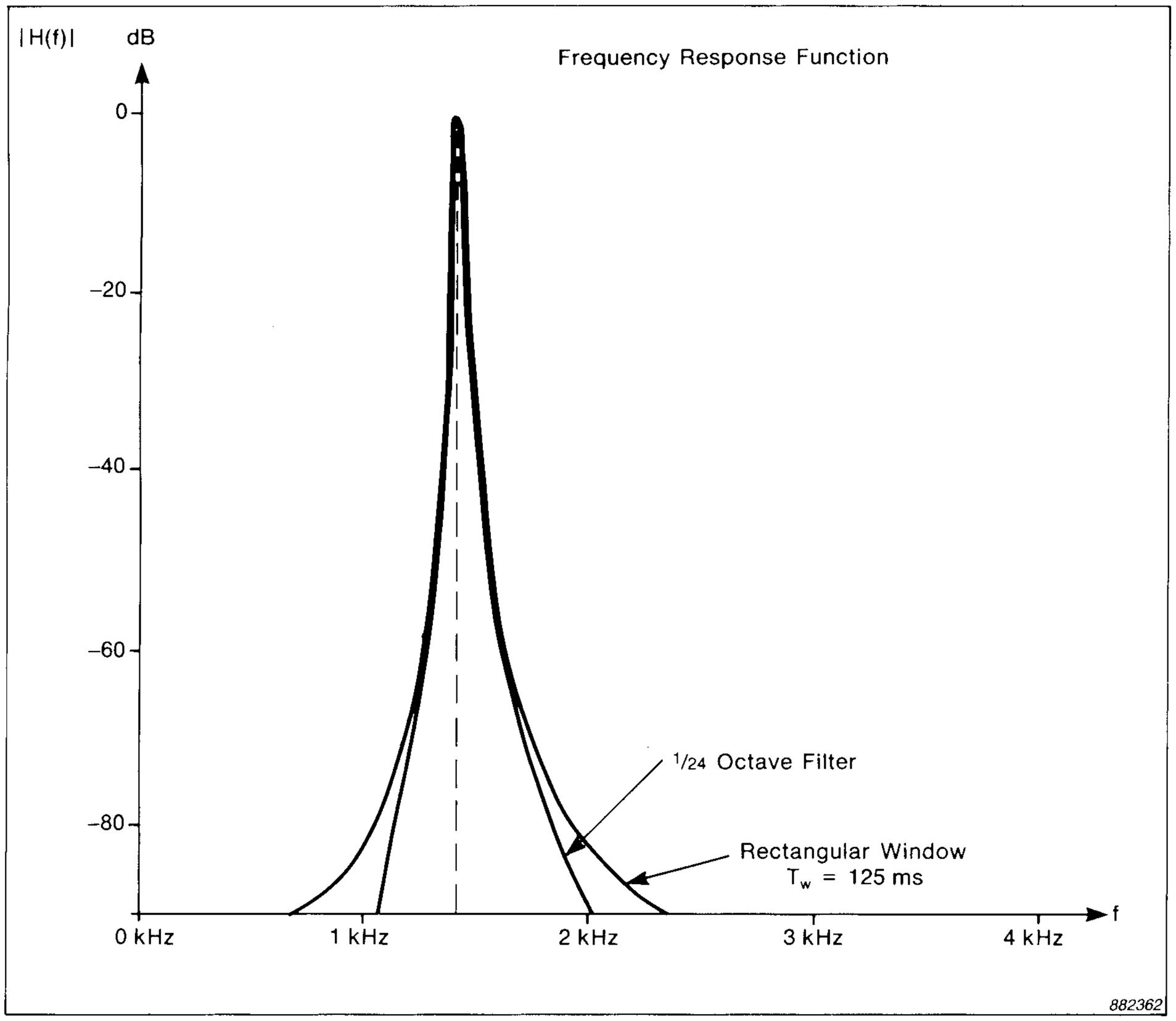

Fig. 12. 1/24 octave filter centred at 1433 Hz using a 125 ms partial filtering time. A minor smearing effect is found at low amplitudes due to a "too short" windowing.

cessing that can be chosen, without lack of confidence in the results will be shown. A short *partial averaging time* is also necessary to achieve a short total averaging time.

In principle we could start the *part-time averaging* of the filter output simultaneously with the start of the *part-time filtering.* On the other hand this would require an unreasonably long averaging time due to the finite rise time of the filter. Therefore, it is better to wait and start the averaging when the filter output has settled. In other words, the *part-time averaging* should start some time after the start of the *part-time filtering,* as indicated in the previous section.

For stationary bandlimited *random signals* $y(t)$, it can be shown that the mean value, $\bar{y}$ and standard deviation, σ are given by

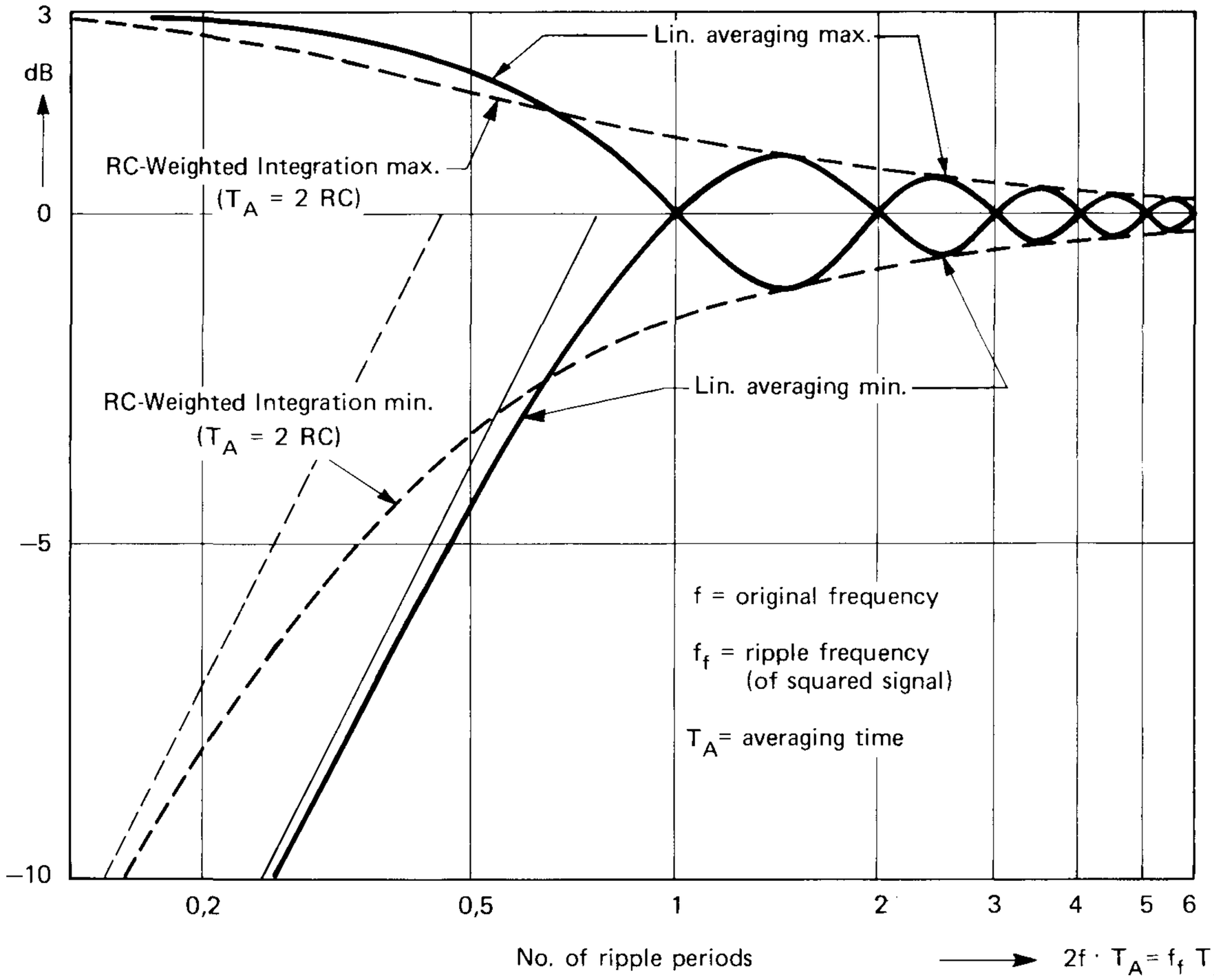

750220/1

Fig. 13. The ripple components for linear and exponential (RC) averaging of squared sinewaves. $T_A = 2RC = 2\tau$ (twice the time constant)

$$\overline{y^2} = \frac{1}{T} \int_T y^2(t)\ \mathrm{dt} \tag{5}$$

$$\sigma \approx \frac{4{,}34}{\sqrt{B \cdot T}}\ [\mathrm{dB}] \tag{6}$$

where B is the filter bandwidth and T is the *total effective averaging time* (Ref. [2]).

This means that it is possible to choose a very short *partial averaging time,* T_{AVG} as long as the averaging takes place over many part intervals.

For stationary *deterministic signals* we have a very different situation. The *partial averaging time,* T_{AVG} has to be so long that the ripple on the partial averaged result is within the specification of accuracy of the analyzer which is ± 0,1 dB.

This is because if we average a *worst* case sinusoidal signal using n non-contiguous time intervals with a *partial averaging time,* T_{AVG} there is no guarantee that the result will be any better than the result after the first partial average.

Let us assume here that a sinusoidal signal with a frequency coinciding with the centre frequency of the filter is analyzed. The output of the filter is squared and averaged using an averaging time of T_A. For linear averaging we will only get a correct result if the averaging time is a multiple of the period time of the squared signal, that is, if half an integer number of periods of the original signal are analyzed (see Fig. 13).

For exponential averaging, a reasonably accurate result is first obtained after many periods (and not necessarily an integer number) of the signal have been analyzed (see Fig. 13).

Since the ripple of the filters in the analysis is specified to be within ± 0,05 dB, the ripple of the averaged sinusoidal signal also has to be within a maximum of ± 0,05 dB after one *partial averaging time* to fulfil the overall specification of ± 0,1 dB.

For exponential averaging we have the following relationship between ripple and averaging time (Ref. [2]):

$$\text{Ripple (dB)} = 10 \log \left(1 \pm \frac{1}{\sqrt{1 + (\pi f T_A)^2}} \right) \text{dB} \qquad (7)$$

Using equation (7) we can calculate the *minimum partial averaging times* for single and dual channel operations as well as 1/12 and 1/24 octave analysis. The results are found in Table 1.

From the results it is seen that the *minimum* required *partial averaging times* are considerably shorter than the *minimum* required *partial filtering times.*

In the Digital Filter Analyzers it has been decided to use *partial averaging times,* T_{AVG} equal to the *minimum partial filtering times* required. This decision has been taken in order to avoid making the relative averaging time too small. This yields *total partial filtering times* that are two times of that indicated in the previous section.

Thus, for single channel 1/12 octave analysis we have that T_{FILT} = 125 ms, T_{AVG} = 62,5 ms and T_{TOT} = 1 s (see Fig. 6). This means that all the non real-time filters are updated on the screen once per second in this measurement mode (see Fig. 7). The results are summarized in Table 2.

Channels	Filter Bandwidth	Centre Frequency	Minimum Partial Averaging Time
1	1/12 octaves	2900 Hz	4,74 ms
2	1/12 octaves	1450 Hz	9,48 ms
1	1/24 octaves	1433 Hz	9,59 ms

T02001GB0

Table 1. Minimum partial averaging times for the three non real-time measurement modes

Octave	*fsamp*	T_{FILT}	T_{AVG}	Samples/T_{FILT}	T_{TOT}
16 kHz	2^{16} Hz	125 ms	62,5 ms	2^{13} = 8192	1 s
8 kHz	2^{15} Hz	125 ms	62,5 ms	2^{12} = 4096	1 s
4 kHz	2^{14} Hz	125 ms	62,5 ms	2^{11} = 2048	1 s

T02002GB0

Table 2. Sampling frequency, total partial filtering time, partial averaging time and the number of processed samples for each filter and the cycle time, for the highest three octaves for non real-time single channel 1/12 octave analysis

Octave	*fsamp*	T_{FILT}	T_{AVG}	Samples/T_{FILT}	T_{TOT}
8 kHz	2^{15} Hz	250 ms	125 ms	8192	2 s
4 kHz	2^{14} Hz	250 ms	125 ms	4096	2 s
2 kHz	2^{13} Hz	250 ms	125 ms	2048	2 s

T02003GB0

Table 3. Sampling frequency, total partial filtering time, partial averaging time, and the number of processed samples for each filter for the highest three octaves for non real-time single channel 1/24 octave and dual channel 1/12 octave analysis

The results for 1/12 octave dual channel and 1/24 octave single channel analysis are summarized in Table 3.

If an upper frequency limit of, for example an 8 kHz octave centre frequency for single channel 1/12 octave analysis is chosen, the above mentioned filtering process is also carried out. The result from the 16 kHz octave band, however, is not displayed or stored.

It should be noted that once the filtering process is initiated it is in progress all the time, whereby the starting point for an averaging can be anywhere within the cycle. Thus the three highest 1/12 octave filters in the 16 kHz octave are not necessarily the first to be updated on the screen.

Examples

The results of single channel 1/12 octave analysis of a white noise random signal are shown in Fig. 14. Only in the case where an averaging time of 1 s (or greater) is used will all of the filters be updated. For a correct scaling of the non real-time filters, an averaging time which is an integer number of the cycle time must be used. For example when using T_A = 1/4 s (Fig. 14a) the non real-time filters have a level which is 4 times (6 dB) too high. This bias error depends on when in the cycle time the filters/detectors are updated. Worst case is a factor of 8 (9 dB). This means that this bias error, ϵ_b will have a maximum value of

$$\epsilon_b = 10 \times \log \left[n/(n-1 + 0{,}125) \right] \text{ dB} \quad (8)$$

where n is the number of cycles chosen in the measurement setup.

This also means that at least 10 cycles must be chosen as the linear averaging time to ensure an error of less than 0,5 dB. This problem can be overcome by setting Special Parameter no. 24 in the General Setup, *Dis-*

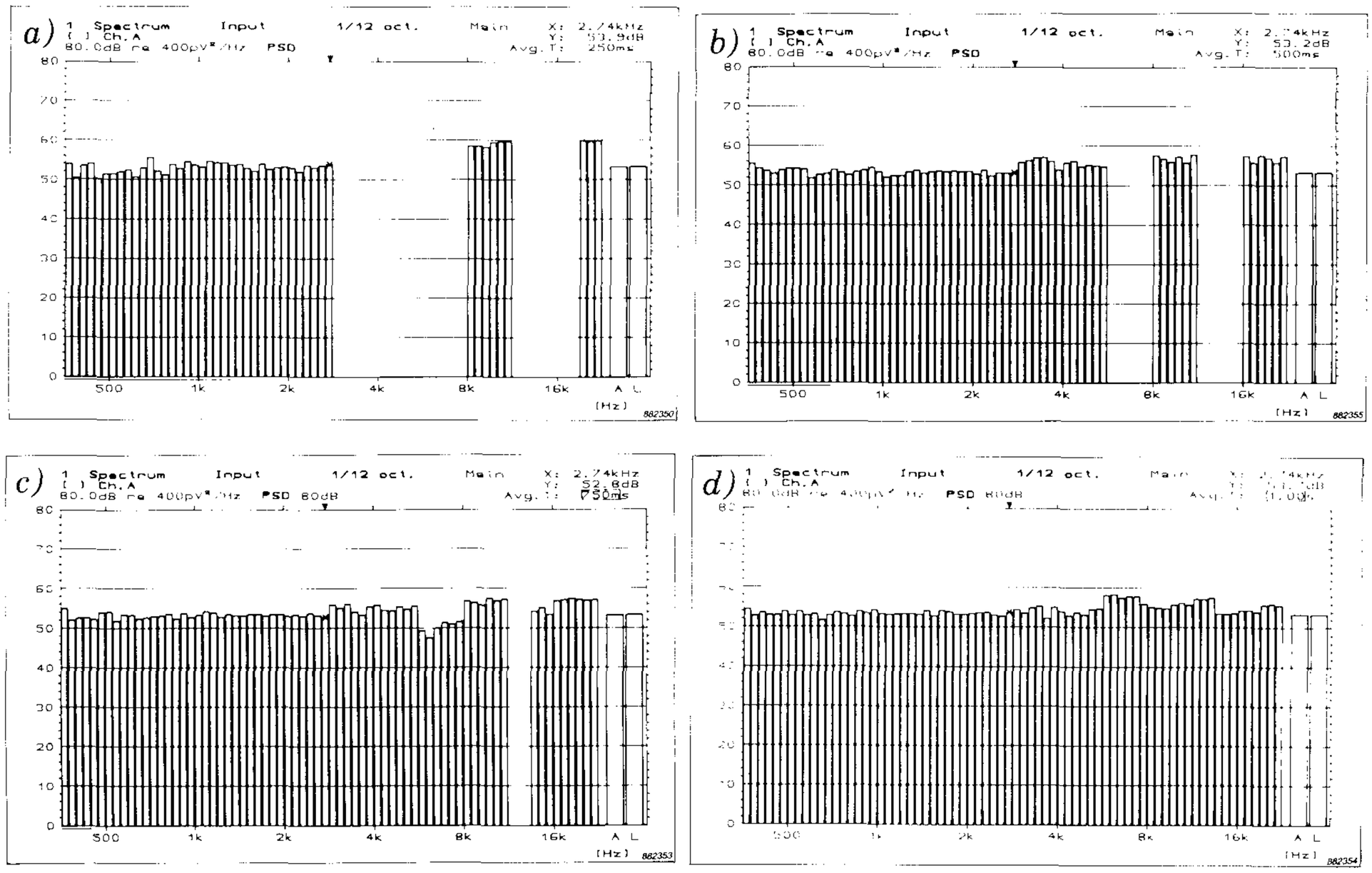

Fig. 14. A stationary white noise random signal analyzed using single channel 1/12 octave analysis. a) Averaging time of 250 ms, b) Averaging time of 500 ms, c) Averaging time of 750 ms, d) Averaging Time of 1 s. Power Spectral Density scaling is used

play of Lin. L_{eq} to *Only Final Values*. In this case all filters are updated at the end of the selected linear averaging time.

For running exponential averaging an averaging time of at least two times the cycle time is sufficient.

Also note that Power Spectral Density (PSD) has been chosen for data representation to give a "horizontal" spectrum rather than the well-known spectrum showing a level increase of 3 dB per octave (see Ref. [4]).

The results of the analysis of 10 short impulses are shown in Fig. 15. The 10 impulses which are regarded here as being one transient were recorded

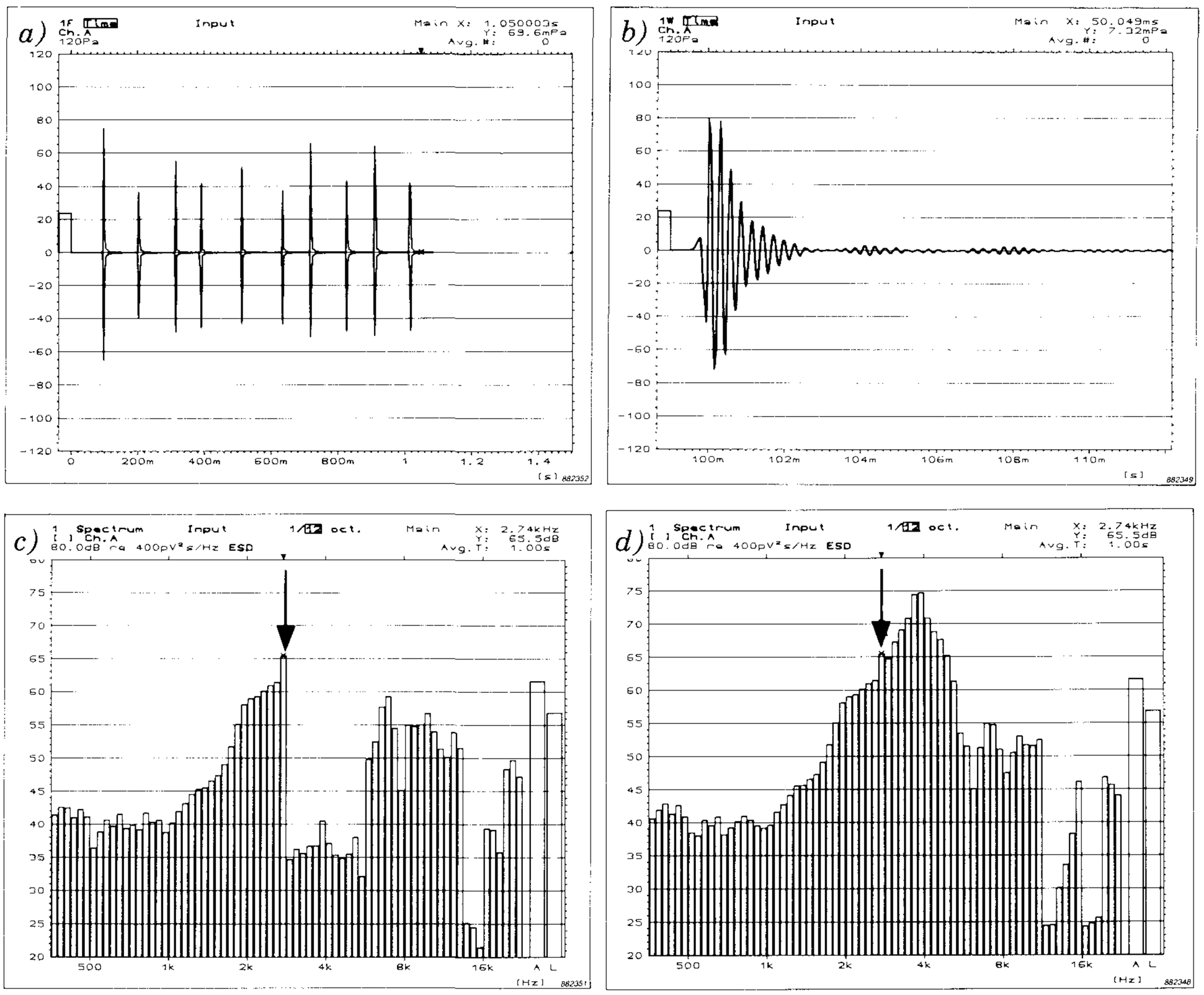

Fig. 15. Analysis of a transient using single channel 1/12 octave analysis up to 16 kHz octave centre frequency
a) 10 impulses to be analyzed
b) One impulse expanded. The period time is approximately 1/4 ms indicating that most of the energy content is found around 4 kHz
c) The transient analyzed using a 1 s averaging time from 0 s to 1 s
d) The transient analyzed using a 1 s averaging time from 0,1 s to 1,1 s

in time mode (Fig. 15a). One impulse is shown in Fig. 15b. The transient was then analyzed from 0s to 1s (Fig. 15c) and from 0,1 s to 1,1 s (Fig. 15d). Notice how the results in the three highest octaves above the 2,74 kHz cursor position are different due to the lack of real-time operation.

Conclusion

It has been shown how the upper frequency limit for 1/12 octave and 1/24 octave digital filter analysis can be extended by two octaves at the cost of losing real-time capacity in the three highest octaves. This mode should only be used when analyzing stationary signals. Furthermore, to ensure correct scaling of all filters, one should either (a) only display the final values for linear averaging or (b) choose an averaging time which is a multiple (at least a factor of 10) of the analysis cycle time. For exponential averaging at least a factor of two times the cycle time has to be chosen as the averaging time. The cycle time is either one or two seconds depending on the measurement mode. The cycle time is also the time interval between each update of the screen for the non real-time filters. It should also be noted that the effective averaging time for these three octaves is 1/16 of the averaging time chosen in the measurement set-up for linear averaging only.

Here it should be noted that with High Frequency Expansion Unit, ZT 0318 installed, the signal processing is always in real-time independent of chosen frequency range and filter bandwidth. The upper frequency limit both in single and dual channel operation with this option is 63 kHz octave centre frequency for both octave and third octave bandwidth analysis. For 1/12 and 1/24 octave bandwidth analysis the upper frequency limits are 16 kHz and 8 kHz octave centre frequencies respectively.

References

[1] Roth, O.: *"Digital Filters in Acoustic Analysis Systems"*, B & K Technical Review, No. 1, 1977

[2] Randall R.B. *"Frequency Analysis"*. B & K, 1987

[3] Rabiner, L.R., Gold, B. *"Theory and Application of Digital Signal Processing"* Prentice-Hall, N.J., 1975

[4] Gade, S., Herlufsen, H.: *"Signal Types and Units"* B & K Technical Review, No.3, 1987

Previously issued numbers of Brüel & Kjær Technical Review

(Continued from cover page 2)

1–1984 Dual Channel FFT Analysis (Part I)
4–1983 Sound Level Meters – The Atlantic Divide
Design principles for Integrating Sound Level Meters
3–1983 Fourier Analysis of Surface Roughness
2–1983 System Analysis and Time Delay Spectrometry (Part II)
1–1983 System Analysis and Time Delay Spectrometry (Part I)
4–1982 Sound Intensity (Part II Instrumentation and Applications)
Flutter Compensation of Tape Recorded Signals for Narrow Band Analysis
3–1982 Sound Intensity (Part I Theory).
2–1982 Thermal Comfort.
1–1982 Human Body Vibration Exposure and its Measurement.
4–1981 Low Frequency Calibration of Acoustical Measurement Systems.
Calibration and Standards. Vibration and Shock Measurements.
3–1981 Cepstrum Analysis.
2–1981 Acoustic Emission Source Location in Theory and in Practice.
1–1981 The Fundamentals of Industrial Balancing Machines and Their Applications.
4–1980 Selection and Use of Microphones for Engine and Aircraft Noise Measurements.
3–1980 Power Based Measurements of Sound Insulation.
Acoustical Measurement of Auditory Tube Opening.
2–1980 Zoom-FFT.
1–1980 Luminance Contrast Measurement.
4–1979 Prepolarized Condenser Microphones for Measurement Purposes.
Impulse Analysis using a Real-Time Digital Filter Analyzer.
3–1979 The Rationale of Dynamic Balancing by Vibration Measurements.
Interfacing Level Recorder Type 2306 to a Digital Computer.
2–1979 Acoustic Emission.
1–1979 The Discrete Fourier Transform and FFT Analyzers.

Special technical literature

Brüel & Kjær publishes a variety of technical literature which can be obtained from your local Brüel & Kjær representative.
The following literature is presently available:

- ○ Mechanical Vibration and Shock Measurements (English), 2nd edition
- ○ Modal Analysis of Large Structures–Multiple Exciter Systems (English)
- ○ Noise Control (English, French)
- ○ Frequency Analysis (English)
- ○ Catalogues (several languages)
- ○ Product Data Sheets (English, German, French, Russian)

Furthermore, back copies of the Technical Review can be supplied as shown in the list above. Older issues may be obtained provided they are still in stock.

Brüel & Kjær

WORLD HEADQUARTERS: DK-2850 Nærum · Denmark
Telephone: +45 42 80 05 00 · Telex: 37316 bruka dk · Fax: +45 42 80 14 05 / +45 42 80 21 63

Australia (02) 450-2066 · Austria 02235/7550*0 · Belgium 02 · 242-97 45 · Brazil (011) 246-8149/246-8166
Canada (514) 695-8225 · Finland (90) 80 17 044 · France (1) 64 57 20 10 · Federal Republic of Germany 04106/70 95-0
Great Britain (01) 954-2366 · Holland 03402-39994 · Hong Kong 5-487486 · Hungary (1) 133 83 05/133 89 29
Italy (02) 52 44 141 · Japan 03-438-0761 · Republic of Korea (02) 554-0605 · Norway 02-90 44 10
Portugal (1) 65 92 56/65 92 80 · Singapore 225 8533 · Spain (91) 268 10 00 · Sweden (08) 711 27 30
Switzerland (042) 65 11 61 · Taiwan (02) 713 9303 · USA (508) 481-7000
Local representatives and service organisations world-wide

ISSN 007–2621
BV 0036–11

PRINTED IN DENMARK BY NÆRUM OFFSET